

## **CHAPTER 2**

# **MECHANICS OF PILE CAP AND PILE GROUP BEHAVIOR**

### **2.1 INTRODUCTION**

The response of a laterally loaded pile within a group of closely spaced piles is often substantially different than a single isolated pile. This difference is attributed to the following three items:

1. The rotational restraint at the pile cap connection. The greater the rotational restraint, the smaller the deflection caused by a given lateral load.
2. The additional lateral resistance provided by the pile cap. As discussed in Chapter 1, verifying and quantifying the cap resistance is the primary focus of this research.
3. The interference that occurs between adjacent piles through the supporting soil. Interference between zones of influence causes a pile within a group to deflect more than a single isolated pile, as a result of pile-soil-pile interaction.

A comprehensive literature review was conducted as part of this research to examine the current state of knowledge regarding pile cap resistance and pile group behavior. Over 350 journal articles and other publications pertaining to lateral resistance, testing, and analysis of pile caps, piles, and pile groups were collected and reviewed.

Pertinent details from these studies were evaluated and, whenever possible, assimilated into tables and charts so that useful trends and similarities can readily be observed. Some of the data, such as graphs that present p-multipliers as functions of pile spacing, are utilized as design aids in subsequent chapters.

This chapter addresses three topics. The first is a review of the current state of practice regarding the lateral resistance of pile caps. The second is a brief review of the most recognized analytical techniques for analysis of single piles. This discussion of single piles is necessary to set the stage for the third topic, which is a review of published field and analytical research conducted to study the behavior of laterally loaded pile groups.

## **2.2 PILE CAP RESISTANCE – STATE OF PRACTICE**

A literature search was performed to establish the state of knowledge with regard to pile cap resistance to lateral loads. The focus of the literature review was directed towards experimental and analytical studies pertaining to the lateral resistance of pile caps, and the interaction of the pile cap with the pile group.

There is a scarcity of published information available in the subject area of pile cap lateral resistance. Of the publications reviewed, only four papers were found that describe load tests performed to investigate the lateral resistance of pile caps. The results from these four studies, summarized in Table 2.1 and Figure 2.1, show that the lateral load resistance provided by pile caps can be very significant, and that in some cases the cap resistance is as large as the resistance provided by the piles themselves.

Beatty (1970) tested two 6-pile groups of step-tapered piles and determined that approximately 50 percent of the applied lateral load was resisted by passive pressure on the pile cap.

Kim and Singh (1974) tested three 6-pile groups of 10BP42 piles and found that removal of soil beneath the pile caps significantly increased the measured deflections, rotations, and bending moments. This effect increased as the load increased.

Rollins et al. (1997) performed static lateral testing on a group of 9 piles and determined the lateral load resistance of the pile cap was greater than the lateral resistance provided by the piles themselves.

Zafir and Vanderpool (1998) tested a group of four drilled shafts, two feet in diameter, embedded in an 11-foot-diameter, 10-foot-thick cap, and determined that the lateral load resistance of the cap was approximately equal to the lateral resistance provided by the drilled shafts. Their measurements showed that the lateral resistance at loads less than 450 tons was provided entirely by passive pressure on the cap.

No systematic method has been reported in the literature for unlinking the cap resistance from the lateral resistance provided by the piles. For the most part, the studies described above addressed only a portion of the cap resistance. For example, the static tests performed by Rollins et al. (1997) considered only the passive resistance at the front of the cap, and only dynamic loads. Kim and Singh (1974) considered only the soil in contact with the bottom of the pile cap. The pile caps in Kim and Singh's study were constructed on the ground surface, and thus the results do not include any passive resistance at the front of the cap or frictional resistance of soil along the sides of the cap. The tests by Beatty (1970) only involved the passive resistance at the front of the cap. The tests by Zafir and Vanderpool (1998) were performed on an atypical pile cap, which consisted of a large, deep circular embedded cap.

These studies indicate that the lateral resistance of pile caps can be quite significant, especially when the pile cap is embedded beneath the ground surface. There is clearly a need for a rational method to evaluate the magnitude of pile cap resistance, and for including this resistance in the design of pile groups to resist lateral loads.

## 2.3 BEHAVIOR OF LATERALLY LOADED SINGLE PILES

Three criteria must be satisfied in the design of pile foundations subjected to lateral forces and moments: 1) the soil should not be stressed beyond its ultimate capacity, 2) deflections should be within acceptable limits, and 3) the structural integrity of the foundation system must be assured.

The first criteria can be addressed during design using ultimate resistance theories such as those by Broms (1964a, 1964b) or Brinch Hansen (1961). The second and third criteria apply to deflections and stresses that occur at working loads. The behavior of piles under working load conditions has been the focus of numerous studies over the past 40 to 50 years. A brief review of the most widely recognized analytical techniques is provided in this section. Many of these techniques can be modified to predict the behavior of closely spaced piles, or pile groups. Modifications for group response are often in the form of empirically or theoretically derived factors that are applied, in various ways, to account for group interaction effects.

Analytical methods for predicting lateral deflections, rotations and stresses in single piles can be grouped under the following four headings:

- Winkler approach,
- p-y method,
- elasticity theory, and
- finite element methods.

These techniques provide a framework for the development of analytical techniques that can be used to evaluate the response of piles in closely spaced groups, which is the subject of Section 2.7.

### 2.3.1 Winkler Approach

The Winkler approach, also called the subgrade reaction theory, is the oldest method for predicting pile deflections and bending moments. The approach uses Winkler's modulus of subgrade reaction concept to model the soil as a series of unconnected linear springs with a stiffness,  $E_s$ , expressed in units of force per length squared ( $FL^{-2}$ ).  $E_s$  is the modulus of soil reaction (or soil modulus) defined as:

$$E_s = \frac{-P}{y} \quad \text{Equation 2.1}$$

where  $p$  is the lateral soil reaction per unit length of the pile, and  $y$  is the lateral deflection of the pile (Matlock and Reese, 1960). The negative sign indicates the direction of soil reaction is opposite to the direction of the pile deflection. Another term that is sometimes used in place of  $E_s$  is the coefficient (or modulus) of horizontal subgrade reaction,  $k_h$ , expressed in units of force per unit volume (Terzaghi 1955). The relationship between  $E_s$  and  $k_h$  can be expressed as:

$$E_s = k_h D \quad \text{Equation 2.2}$$

where  $D$  is the diameter or width of the pile.  $E_s$  is a more fundamental soil property because it is not dependent on the pile size. The behavior of a single pile can be analyzed using the equation of an elastic beam supported on an elastic foundation (Hetenyi 1946), which is represented by the 4<sup>th</sup> order differential beam bending equation:

$$E_p I_p \frac{d^4 y}{dx^4} + Q \frac{d^2 y}{dx^2} + E_s y = 0 \quad \text{Equation 2.3}$$

where  $E_p$  is the modulus of elasticity of the pile,  $I_p$  is the moment of inertia of the pile section,  $Q$  is the axial load on the pile,  $x$  is the vertical depth, and  $y$  is the lateral deflection of the pile at point  $x$  along the length of the pile.

The governing equation for the deflection of a laterally loaded pile, obtained by applying variational techniques (minimization of potential energy) to the beam bending equation (Reddy 1993), and ignoring the axial component, is:

$$\frac{d^4 y}{dx^4} + \frac{E_s}{E_p I_p} y = 0 \quad \text{Equation 2.4}$$

Solutions to Equation 2.4 have been obtained by making simplifying assumptions regarding the variation of  $E_s$  (or  $k_h$ ) with depth. The most common assumption is that  $E_s$  is constant with depth for clays and  $E_s$  varies linearly with depth for sands. Poulos and Davis (1980) and Prakash and Sharma (1990) provide tables and charts that can be used to determine pile deflections, slopes, and moments as a function of depth and non-dimensional coefficients for a constant value of  $E_s$  with depth.

The soil modulus for sand and normally consolidated clay is often assumed to vary linearly with depth, as follows:

$$E_s = kx \quad \text{Equation 2.5}$$

where  $k$  (defined using the symbol  $n_h$  by Terzaghi, 1955) is the constant of horizontal subgrade reaction, in units force per volume. For this linear variation of  $E_s$  with depth, Matlock and Reese (1960) and Poulos and Davis (1980) present nondimensional coefficients that can be used to calculate pile deflections, rotations, and bending moments for various pile-head boundary conditions. Gill and Demars (1970) present other formulations for the variation of  $E_s$  with depth, such as step functions, hyperbolic functions, and exponential functions.

The subgrade reaction method is widely employed in practice because it has a long history of use, and because it is relatively straight forward to apply using available chart and tabulated solutions, particularly for a constant or linear variation of  $E_s$  with depth. Despite its frequent use, the method is often criticized because of its theoretical shortcomings and limitations. The primary shortcomings are:

1. the modulus of subgrade reaction is not a unique property of the soil, but depends intrinsically on pile characteristics and the magnitude of deflection,
2. the method is semi-empirical in nature,
3. axial load effects are ignored, and
4. the soil model used in the technique is discontinuous. That is, the linearly elastic Winkler springs behave independently and thus displacements at a point are not influenced by displacements or stresses at other points along the pile (Jamiolkowski and Garassino 1977).

Modifications to the original subgrade reaction approach have been proposed to account for some of these shortcomings. One of these modifications attempts to convert the Winkler model to a continuous model by coupling the springs using an inter-spring shear layer component (Georgiadis and Butterfield 1982). This model also accounts for the contribution of edge shear along the pile boundaries. The model has not gained widespread acceptance because of difficulties associated with obtaining soil parameters necessary to develop coefficients for use in the model (Horvath 1984).

McClelland and Focht (1956) augmented the subgrade reaction approach using finite difference techniques to solve the beam bending equation with nonlinear load versus deflection curves to model the soil. Their approach is known as the  $p$ - $y$  method of analysis. This method has gained popularity in recent years with the availability of powerful personal computers and commercial software such as COM624 (1993) and LPILE Plus3.0 (1997). A brief summary of the  $p$ - $y$  method of analysis is presented in the following section.

### 2.3.2 $p$ - $y$ Method of Analysis

The  $p$ - $y$  approach for analyzing the response of laterally loaded piles is essentially a modification or “evolutionary refinement” (Horvath 1984) of the basic Winkler model, where  $p$  is the soil pressure per unit length of pile and  $y$  is the pile deflection. The soil is represented by a series of nonlinear  $p$ - $y$  curves that vary with depth and soil type. An example of a hypothetical  $p$ - $y$  model is shown in Figure 2.2 (a).

The method is semi-empirical in nature because the shape of the  $p$ - $y$  curves is determined from field load tests. Reese (1977) has developed a number of empirical or “default” curves for typical soil types based on the results of field measurements on fully instrumented piles. The most widely used analytical expression for  $p$ - $y$  curves is the cubic parabola, represented by the following equation:

$$\frac{p}{p_{ult}} = 0.5 \left( \frac{y}{y_{50}} \right)^{\frac{1}{3}} \quad \text{Equation 2.6}$$

where  $p_{ult}$  is the ultimate soil resistance per unit length of pile and  $y_{50}$  is the deflection at one-half the ultimate soil resistance. To convert from strains measured in laboratory triaxial tests to pile deflections, the following relationship is used for  $y_{50}$ :

$$y_{50} = A e_{50} D \quad \text{Equation 2.7}$$

where  $e_{50}$  is the strain at  $\frac{1}{2}$  the maximum principal stress difference, determined in a laboratory triaxial test,  $D$  is the pile width or diameter, and  $A$  is a constant that varies from 0.35 to 3.0 (Reese 1980).

The deflections, rotations, and bending moments in the pile are calculated by solving the beam bending equation using finite difference or finite element numerical techniques. The pile is divided into a number of small increments and analyzed using  $p$ - $y$  curves to represent the soil resistance.



In this representation, the axial load in the pile,  $Q$ , is implicitly assumed constant with depth, to simplify computations. This assumption does not adversely effect the analysis because  $Q$  has very little effect on the deflection and bending moment. Furthermore, the maximum bending moment is generally only a relatively short distance below the groundline, or pile cap, where the value of  $Q$  is undiminished (Reese, 1977).

Four additional equations are necessary to balance the number of equations and the number of unknowns in the finite difference formulation. These four equations are represented by boundary conditions, two at the pile top and two at the bottom of the pile. At the bottom of the pile, one boundary condition is obtained by assuming a value of zero moment, or:

$$EI \left( \frac{d^2 y}{dx^2} \right) = 0 \quad \text{Equation 2.8}$$

The second boundary condition at the pile bottom involves specifying the shear of the pile using the following expression at  $x = L$ :

$$EI \left( \frac{d^3 y}{dx^3} \right) + Q \left( \frac{dy}{dx} \right) = V \quad \text{Equation 2.9}$$

where  $V$  is the shear force, which is usually set equal to zero for long piles.

The two boundary conditions at the top of the pile depend on the shear, moment, rotation, and displacement circumstances at the pile top. These are generalized into the following four categories:

1. Pile not restrained against rotation. This is divided into two subcategories: (a) “flagpole” and (b) free-head conditions.

2. Vertical load applied eccentrically at the ground surface (moment loading condition).
3. Pile head extends into a superstructure or is partially restrained against rotation (partially restrained condition).
4. Pile head rotation is known, usually assumed = 0 (fixed-head condition).

Category	Shear V	Moment M	Rotation $\theta$	Displacement y
1(a). free-head - "flagpole"	known ( $> 0$ )	known ( $> 0$ at groundline)	unknown ( $> 0$ )	unknown ( $> 0$ )
1(b). free-head - pinned	known ( $> 0$ )	known ( $= 0$ )	unknown ( $> 0$ )	unknown ( $> 0$ )
2. moment loading	known ( $= 0$ )	known ( $> 0$ )	unknown ( $> 0$ )	unknown ( $> 0$ )
3. partially restrained	known ( $> 0$ )	M/ $\theta$ known	M/ $\theta$ known	unknown ( $> 0$ )
4. fixed-head	known ( $> 0$ )	unknown ( $< 0$ )	known ( $= 0$ )	unknown ( $> 0$ )

The  $p$ - $y$  method is readily adapted to computer implementation and is available commercially in the computer programs LPILEPlus 3.0 (1997) and COM624 (1993). The method is an improvement over the subgrade reaction approach because it accounts for the nonlinear behavior of most soils without the numerical limitations inherent in the subgrade reaction approach. However, the method has some limitations, as described below:

1. The  $p$ - $y$  curves are independent of one another.  
Therefore, the continuous nature of soil along the length of the pile is not explicitly modeled.

2. Suitable  $p$ - $y$  curves are required. Obtaining the appropriate  $p$ - $y$  curve is analogous to obtaining the appropriate value of  $E_s$ ; one must either perform full-scale instrumented lateral load tests or adapt the existing available standard curves (default curves) for use in untested conditions. These default curves are limited to the soil types in which they were developed; they are not universal.
3. A computer is required to perform the analysis.

Other representations of  $p$ - $y$  curves have been proposed such as the hyperbolic shape by (Kondner 1963). Evans (1982) and Mokwa et al. (1997) present a means of adjusting the shape of the  $p$ - $y$  curve to model the behavior of soils that have both cohesion and friction using Brinch Hansen's (1961)  $f$ - $c$  ultimate theory. In situ tests such as the dilatometer (Gabr 1994), cone penetrometer (Robertson et al. 1985), and pressuremeter (Ruesta and Townsend 1997) have also been used to develop  $p$ - $y$  curves.

### 2.3.3 Elasticity Theory

Poulos (1971a, 1971b) presented the first systematic approach for analyzing the behavior of laterally loaded piles and pile groups using the theory of elasticity. Because the soil is represented as an elastic continuum, the approach is applicable for analyzing battered piles, pile groups of any shape and dimension, layered systems, and systems in which the soil modulus varies with depth. The method can be adapted to account for the nonlinear behavior of soil and provides a means of determining both immediate and final total movements of the pile (Poulos 1980).

Poulos's (1971a, 1971b) method assumes the soil is an ideal, elastic, homogeneous, isotropic semi-infinite mass, having elastic parameters  $E_s$  and  $\nu_s$ . The pile is idealized as a thin beam, with horizontal pile deflections evaluated from integration of

the classic Mindlin equation for horizontal subsurface loading. The Mindlin equation is used to solve for horizontal displacements caused by a horizontal point load within the interior of a semi-infinite elastic-isotropic homogeneous mass. Solutions are obtained by integrating the equation over a rectangular area within the mass. The principle of superposition is used to obtain displacement of any points within the rectangular area. Details of the Mindlin equation can be found in Appendix B of *Pile Foundation Analysis and Design* by Poulos and Davis (1980).

The pile is assumed to be a vertical strip of length  $L$ , width  $D$  (or diameter,  $D$ , for a circular pile), and flexural stiffness  $E_p I_p$ . It is divided into  $n+1$  elements and each element is acted upon by a uniform horizontal stress  $p$ . The horizontal displacements of the pile are equal to the horizontal displacements of the soil. The soil displacements are expressed as:

$$\{y_s\} = \frac{d}{E_s} [I_s] \{p\} \quad \text{Equation 2.10}$$

where  $\{y_s\}$  is the column vector of soil displacements,  $\{p\}$  is the column vector of horizontal loading between soil and pile, and  $[I_s]$  is the  $n+1$  by  $n+1$  matrix of soil-displacement influence factors determined by integrating Mindlin's equation, using boundary element analyses (Poulos 1971a). The finite difference form of the beam bending equation is used to determine the pile displacements. The form of the equation varies depending on the pile-head boundary conditions. Poulos and Davis (1980) present expressions for free-head and fixed-head piles for a number of different soil and loading conditions. One of the biggest limitations of the method (in addition to computational complexities) is the difficulty in determining an appropriate soil modulus,  $E_s$ .

### 2.3.4 Finite Element Method

The finite element method is a numerical approach based on elastic continuum theory that can be used to model pile-soil-pile interaction by considering the soil as a three-dimensional, quasi-elastic continuum. Finite element techniques have been used to

analyze complicated loading conditions on important projects and for research purposes. Salient features of this powerful method include the ability to apply any combination of axial, torsion, and lateral loads; the capability of considering the nonlinear behavior of structure and soil; and the potential to model pile-soil-pile-structure interactions. Time-dependent results can be obtained and more intricate conditions such as battered piles, slopes, excavations, tie-backs, and construction sequencing can be modeled. The method can be used with a variety of soil stress-strain relationships, and is suitable for analyzing pile group behavior, as described in Section 2.7.5. Performing three-dimensional finite element analyses requires considerable engineering time for generating input and interpreting results. For this reason, the finite element method has predominately been used for research on pile group behavior, rarely for design.

## **2.4 PILE GROUP BEHAVIOR – EXPERIMENTAL RESEARCH**

### **2.4.1 Background**

The literature review also encompassed the current state of practice in the area of pile group behavior and pile group efficiencies. This section describes relevant aspects of experimental studies reported in the literature. Analytical studies of pile group behavior are described in Section 2.7.

Table A.1 (located in Appendix A) contains a summary of 37 experimental studies in which the effects of pile group behavior were observed and measured. The table includes many relevant load tests that have been performed on pile groups during the past 60 years. The references are organized chronologically. Multiple references indicate that a particular test was addressed in more than one published paper.

The conventions and terms used to describe pile groups in this dissertation are shown in Figure 2.3. Most pile groups used in practice fall into one of the following three categories, based on the geometric arrangement of the piles:

1. Figure 2.3 (a) – **in-line arrangement**. The piles are aligned in the direction of load.
2. Figure 2.3 (b) – **side-by-side arrangement**. The piles are aligned normal to the direction of load.
3. Figure 2.3 (c)– **box arrangement**. Consists of multiple in-line or side-by-side arrangements.

Pile rows are labeled as shown in Figure 2.3(c). The leading row is the first row on the right, where the lateral load acts from left to right. The rows following the leading row are labeled as 1<sup>st</sup> trailing row, 2<sup>nd</sup> trailing row, and so on. The spacing between two adjacent piles in a group is commonly described by the center to center spacing, measured either parallel or perpendicular to the direction of applied load. Pile spacings are often normalized by the pile diameter,  $D$ . Thus, a spacing identified as  $3D$  indicates the center to center spacing in a group is three times the pile diameter. This convention is used throughout this document.

The experimental studies described in Table A1 are categorized under three headings:

1. full-scale field tests (15 studies)
2. 1g model tests (16 studies)
3. geotechnical centrifuge tests (6 studies)

Pertinent details and relevant test results are discussed in the following sections.

#### **2.4.2 Full-Scale Field Tests**

Full-scale tests identified during the literature review include a wide variety of pile types, installation methods, soil conditions, and pile-head boundary conditions, as shown in Table 2.2.

The earliest reported studies (those by Feagin and Gleser) describe the results of full-scale field tests conducted in conjunction with the design and construction of large pile-supported locks and dams along the Mississippi River. O'Halloran (1953) reported tests that were conducted in 1928 for a large paper mill located in Quebec City, Canada, along the banks of the St. Charles River. Load tests performed in conjunction with the Arkansas River Navigation Project provided significant amounts of noteworthy design and research data, which contributed to advancements in the state of practice in the early 1970's. Alizadeh and Davisson (1970) reported the results of numerous full-scale lateral load tests conducted for navigation locks and dams that were associated with this massive project, located in the Arkansas River Valley.

Ingenious methods were devised in these tests for applying loads and monitoring deflections of piles and pile groups. The load tests were usually conducted during design and, very often, additional tests were conducted during construction to verify design assumptions. In many instances, the tests were performed on production piles, which were eventually integrated into the final foundation system.

The most notable difference between the tests conducted prior to the 1960's and those conducted more recently is the sophistication of the monitoring instruments. Applied loads and pile-head deflection were usually the only variables measured in the earlier tests. Loads were typically measured manually by recording the pressure gauge reading of the hydraulic jack.

A variety of methods were employed to measure deflections. In most cases, more than one system was used to provide redundancy. For example, Feagin (1953) used two completely independent systems. One system used transit and level survey instruments, and the other system consisted of micrometers, which were embedded in concrete and connected to piano wires under 50 pound of tension. Electronic contact signals were used to make the measurements with a galvanometer connected in series with a battery. O'Halloran (1953) manually measured horizontal deflections using piano wire as a point of reference. The piano wires, which were mounted outside the zone of influence of the

test, were stretched across the centerline of each pile, at right angles to the direction of applied load. Deflection measurements were made after each load application by measuring the horizontal relative displacement between the pile center and the piano wire.

Over the last 30 to 40 years, the level of sophistication and overall capabilities of field monitoring systems have increased with the advent of personal computers and portable multi-channel data acquisition systems. Hydraulic rams or jacks are still commonly used for applying lateral loads for static testing. However, more advanced systems are now used for cyclic and dynamic testing. Computer-driven servo-controllers are often used for applying large numbers of cyclic loads. For example, Brown and Reese (1985) applied 100 to 200 cycles of push-pull loading at 0.067 Hz using an MTS servo valve operated by an electro-hydraulic servo controller.

A variety of methods have been used to apply dynamic loads. Blaney and O'Neill (1989) used a linear inertial mass vibrator to apply dynamic loads to a 9-pile group at frequencies as high as 50 Hz. Rollins et al. (1997) used a statnamic loading device to apply large loads of short duration (100 to 250 msec) to their test pile group. The statnamic device produces force by igniting solid fuel propellant inside a cylinder (piston), which causes a rapid expansion of high-pressure gas that propels the piston and forces the silencer and reaction mass away.

Powerful electronic systems are now available to facilitate data collection. These systems usually have multiple channels for reading responses from a variety of instruments at the same time. It is now possible to collect vast amounts of information during a test at virtually any frequency and at resolutions considerably smaller than is possible using optical or mechanical devices.

Pile deflections and rotations are often measured using displacement transducers, linear potentiometers, and linear variable differential transformers (LVDT's). In addition to measuring deflections, piles are often instrumented with strain gauges and slope



inclinometers. Information obtained from these devices can be used to calculate stresses, bending moments, and deflections along the length of a pile.

Whenever possible, strain gauges are installed after the piles are driven to minimize damage. A technique commonly used with closed-end pipe piles is to attach strain gauges to a smaller diameter steel pipe or sister bar, which is then inserted into the previously driven pile and grouted in place. This method was used in the tests performed on pipe piles by Brown (1985), Ruesta and Townsend (1997), and Rollins et al. (1998).

In some cases, strain gauges are attached prior to installing piles. For instance, gauges are often attached to steel H-piles prior to driving; or gauges may be attached to the reinforcing steel cage prior to pouring concrete for bored piles (drilled shafts). Meimon et al. (1986) mounted strain gauges on the inside face of the pile flange and mounted a slope inclinometer tube on the web face. They protected the instruments by welding steel plates across the ends of the flanges creating a boxed-in cross-section, and drove the piles close-ended.

Applied loads are usually measured using load cells. Ruesta and Townsend (1997) used ten load cells for tests on a 9-pile group. One load cell was used to measure the total applied load, and additional load cells were attached to the strut connections at each pile. Additional instruments such as accelerometers, geophones, and earth pressure cells are sometimes used for specialized applications.

### **2.4.3 1g Model Tests**

The majority of experiments performed on pile groups fall under the category of 1g model tests. Model tests are relatively inexpensive and can be conducted under controlled laboratory conditions. This provides an efficient means of investigation. For instance, Cox et al. (1984) reported on a study in which tests on 58 single piles and 41 pile groups were performed. They varied the geometric arrangement of piles within groups, the number of piles per group, and the spacing between piles. Liu (1991) performed 28 sets of tests on pile groups in which the pile spacing, group configuration,

and pile lengths were varied. Franke (1988) performed a number of parametric studies by varying the arrangement, size, and spacing of piles within groups; the length and stiffness of the piles; the pile head boundary conditions; and the relative density of the backfill soil.

Aluminum is the most frequently used material for fabricating model piles. Small diameter aluminum pipes, bars, or tubes were used in 8 of the 16 model tests reported in Table A.1. Other materials such as mild steel and chloridized-vinyl (Shibata et al. 1989) have also been used. Tschebotarioff (1953) and Wen (1955) used small wood dowels to represent timber piles in their model tests

Sand was by far the most commonly used soil (12 out of 16 tests); however, silt and clay soils were used as well. A variety of techniques were used to place soil and install piles. In some studies, soil was placed first and the piles were subsequently driven, pushed or bored into place. In other cases, the piles were held in place as soil was placed around them. Techniques for installing soil included tamping, pluviation, raining, dropping, flooding, and “boiling”. Shibata et al. (1989) applied the term boiling to the technique of pumping water with a strong upward gradient through the bottom of a sand-filled tank.

The primary shortcomings of 1g model testing are related to scaling and edge effects. Scaling effects limit the applicability of model tests in simulating the performance of prototypes. Models are useful in performing parametric studies to examine relative effects, but it is appropriate to exercise caution in extrapolating results obtained from model tests to full-scale dimensions. Items such as at-rest stress levels, soil pressure distributions, and soil particle movements are all factors influenced by scaling (Zhang and Hu 1991).

Edge effects become significant if the size of the test tank is too small relative to the size of the model pile. Prakash (1962) reported the results of tests in a large test tank in which the zone of influence (or zone of interference) extended a distance of 8 to 12

times the pile width in the direction of loading and 3 to 4 times the pile width normal to the direction of loading. Experimental apparatus that do not meet these guidelines would involve edge effects, which are not easily quantified.

As discussed in the following paragraphs, centrifuge tests have become increasingly popular in the last decade as a means of overcoming scaling effects inherent in 1g model testing.

#### **2.4.4 Centrifuge Tests**

Similar to 1g model testing, a geotechnical centrifuge provides a relatively rapid method for performing parametric studies. The advantage of centrifuge modeling lies in the ability of the centrifuge to reproduce prototype stress-strain conditions in a reduced scale model (McVay et al. 1995).

For additional information pertaining to centrifuge mechanics, the reader is referred to the 20<sup>th</sup> Rankine Lecture by Schofield (1980), which provides a detailed discussion of centrifuge testing principles. Schofield explains the mechanics behind centrifuge modeling in terms of Newtonian physics and the theory of relativity. In essence, the gravitational force of a prototype body is indistinguishable from, and identical to, an inertial force created in the centrifuge. Thus, if the product of depth times acceleration is the same in model and prototype, the stresses at every point within the model will theoretically be the same as the stresses at every corresponding point in the prototype (Schofield 1980).

Four studies that investigated the lateral resistance of pile groups using geotechnical centrifuges were found during the literature study, and these are summarized in Table A.1. Some details about the facilities are provided in Table 2.3. Significant aspects of the studies are discussed in the following paragraphs.

The first centrifuge tests on model pile groups were performed by Barton (1984) on groups consisting of 2, 3, and 6 piles at various spacings and orientations with respect

to the direction of load. Zhang and Hu (1991) examined the effect of residual stresses on the behavior of laterally loaded piles and pile groups. Adachi et al. (1994b) examined pile-soil-pile interaction effects by testing two piles at various spacings and orientations. In these three studies, the soil was placed and the piles were installed prior to starting the centrifuge (i.e., pile installation occurred at 1g).

McVay et al. (1994) was the first to install pile groups in flight, laterally load them, and measure their response without stopping the centrifuge. The results from McVay's study indicates that piles have greater resistance to lateral and axial loads when driven at prototype stress levels (centrifuge in motion during pile installation), as opposed to 1g installation. The difference in behavior is attributed to the significantly greater dilation of the test sand at 1g and resulting decrease in density and strength (McVay et al. 1995).

McVay et al. (1994, 1995, and 1998) measured group efficiencies and back-calculated p-multipliers for pile groups ranging in size from 3 by 3 to 3 by 7 (3 rows oriented parallel to the direction of loading and 7 rows oriented normal to the direction of load). Spacings of 3 and 5 times the pile diameter were tested using both loose- and medium-dense sand backfill.

Centrifuge testing appears to provide a relatively efficient means of systematically investigating several variables at prototype stress conditions. Factors that impact centrifuge test results include boundary conditions or edge effects between the model foundation and the centrifuge bucket (model container), and soil behavior incongruities caused by installing piles at 1g, rather than in flight. Additional inconsistencies between model and prototype behavior may arise when testing clayey soils. Schofield (1980) describes these limitations and attributes them to changes in water contents, pore pressures, and equivalent liquidities, which are difficult to model in the centrifuge.

## 2.5 PILE GROUP EFFICIENCY

### 2.5.1 Background

Piles are usually constructed in groups and tied together by a concrete cap at the ground surface. Piles in closely spaced groups behave differently than single isolated piles because of pile-soil-pile interactions that take place in the group. It is generally recognized that deflections of a pile in a closely spaced group are greater than the deflections of an individual pile at the same load because of these interaction effects. The maximum bending moment in a group will also be larger than that for a single pile, because the soil behaves as if it has less resistance, allowing the group to deflect more for the same load per pile.

The most widely recognized standard for quantifying group interaction effects is the group efficiency factor,  $G_e$ , which is defined in Equation 2.11 as the average lateral capacity per pile in a group divided by the lateral capacity of a single pile (Prakash 1990).

$$G_e = \frac{(Q_u)_g}{n(Q_u)_s} \quad \text{Equation 2.11}$$

Where  $(Q_u)_g$  is the ultimate lateral load capacity of the group,  $n$  is the number of piles in the group, and  $(Q_u)_s$  is the ultimate lateral load capacity of a single pile. A somewhat different definition for the group efficiency factor, one that is based on p-multipliers, is described in Section 2.6.

The analysis of pile group behavior can be divided into widely-spaced closely-spaced piles. Model tests and a limited number of full-scale tests indicate that piles are not influenced by group effects if they are spaced far apart.

Piles installed in groups at close spacings will deflect more than a single pile subjected to the same lateral load per pile because of group effects (Bogard and Matlock, 1983). There is general agreement in the literature that group effects are small when

center-to-center pile spacings exceed 6 pile diameters (6D) in a direction parallel to the load and when they exceed 3D measured in a direction perpendicular to the load. This approximation has been validated through experimental tests by Prakash (1967), Franke (1988), Lieng (1989), and Rao et al. (1996).

Group efficiency factors can be evaluated experimentally by performing load tests on pile groups and on comparable single piles. The next section summarizes over 60 years of experimental research in the area of pile group efficiencies.

### 2.5.2 Group Efficiency Factors

Fourteen of the studies included in Table A.1 involve experimental evaluations of the group efficiency factor,  $G_e$ , or provide enough information to calculate  $G_e$  using Equation 2.11. The references for these 14 studies are tabulated chronologically in Table 2.4. Pertinent data from these papers are presented in Table 2.4 for three geometric arrangements, defined in Figure 2.3 as: box, in-line, and side-by-side. Some of the references, such as Cox et al. (1984) and Shibata et al. (1989), include multiple tests conducted using different geometric arrangements and pile spacings. For clarity, these tests were arranged into separate rows of the table. Of the 85 separate tests described in Table 2.4, only five percent (4 tests) were full-scale. The remaining tests were performed on reduced scale models, either 1g model or centrifuge. The large percentage of model tests is due to the relative ease and lower cost of these tests, as opposed to full-scale field tests.

The studies summarized in Table 2.4 were examined in detail to determine the factors that most significantly effect overall group efficiency. Because most of these factors are interrelated, those with greatest significance are identified first. In order of importance, these factors are:

- pile spacing
- group arrangement

- group size
- pile-head fixity
- soil type and density
- pile displacement

### ***Pile Spacing***

Center to center pile spacing is the dominant factor affecting pile group efficiency. Cox et al. (1984) measured group efficiencies ranging from 0.59 at 1.5D spacing to 0.95 at 3D spacing for a 3-pile in-line arrangement in very soft clay. For the same arrangement of piles in medium dense sand, Sarsby (1985) reported nearly the same values of group efficiencies ranging from 0.66 at 2D spacing to 0.80 at 8D spacing.

The results for all of the tests summarized in Table 2.4, are plotted in Figure 2.4 as a function of center to center pile spacing. The most significant trend in this figure is the increase of  $G_e$  with pile spacing. However, there is a large amount of scatter in the data indicating that other factors also influence the value of  $G_e$ . To estimate accurate values of group efficiency, it is necessary to consider factors in addition to pile spacing.

### ***Group Arrangement and Group Size***

After pile spacing, the next most significant factor appears to be the geometric arrangement of piles within the group. Observable trends are evident in Figure 2.4, where the group arrangements (square, in-line, and side-by-side) are delineated using different symbols. Piles in square arrangements are represented by solid squares, in-line arrangements are identified by solid circles, and side-by-side arrangements are identified by open circles. The three outlying data points (shown as solid circles) at 8D spacing represent results from Sarsby's (1985) 1g model tests. These tests were performed on small (less than 1/4-inch-diameter) steel bars. The bars were repeatedly pushed laterally to deflections greater than 20 times the pile diameter, and  $G_e$  values were determined by extrapolating the resistance curves back to zero deflection. Because the test procedure is

questionable, and the results are not consistent with those from other more reasonable test procedures, no weight is placed on these tests in the development of recommendations for design.

For clarity, the test results are plotted and described separately based on the arrangement of piles within a group, as follows:

- box arrangement - Figures 2.5 and 2.6
- in-line arrangement – Figures 2.7 and 2.8
- side-by-side arrangement - Figure 2.9

Design curves were visually fitted through the data points for the three types of pile arrangements, using engineering judgement, as described below.

**Box arrangement.** Test results from Table 2.4 for multiple rows of piles oriented in box arrangements are plotted in Figure 2.5, along with the proposed design curve. The design curve is linear between  $G_e = 1.0$  at a spacing of  $6D$ , and  $G_e = 0.25$  at a spacing of  $1D$ .

There is no clear effect of group size, as can be seen in Figure 2.6. This may be a result of scatter in the data. One could logically infer that shadowing effects would increase with group size. If this were the case, group efficiency would be expected to decrease as group size increased. As additional data becomes available, it may be possible to quantify the effect of group size.

**In-line arrangement.** Test results from Table 2.4 for single rows of piles oriented in the direction of load (in-line arrangement) are plotted in Figure 2.7, along with proposed design lines. Based on this plot, it can be noted that group efficiency is influenced by the number of piles in the line. This can be seen more clearly in Figure 2.8, where the data points are plotted using symbols that indicate the number of piles per line, either 2, 3, or 4. The following conclusions can be drawn from this plot:



1. At the same pile spacing, a single row of in-line piles will have a greater group efficiency than piles in a box arrangement.
2. At a given spacing, the group efficiency decreases as the number of piles in a line increase.

As additional data become available, it may be possible to refine the design lines shown in Figures 2.7 and 2.8.

**Side-by-side arrangement.** Test results from Table 2.4 for single rows of piles oriented normal to the direction of load (side-by-side arrangement) are plotted in Figure 2.9, along with the proposed design line. From this plot, it is concluded that:

1. Piles oriented in side-by-side arrangements are effected by pile spacing to a lesser degree than in-line or box arrangements of piles.
2. For practical purposes, side-by-side piles spaced at 3D or greater experience no group effects. In other words, side-by-side piles spaced at 3D or greater will behave the same as single isolated piles.

### ***Pile Head Fixity***

Approximately 80 % of the tests described in Table 2.4 were reportedly performed on free-headed piles, with either pinned or “flag pole” boundary conditions. The remaining 20 % of the tests were performed on piles with fixed-head boundary conditions. It is postulated, that the boundary conditions for some of the tests reported in Table 2.4 were partially restrained, rather than fixed or free headed. Significant conclusions regarding the impact of pile head restraint on group efficiency are not possible because of inconsistencies regarding the classification of boundary conditions and the small number of fixed-headed tests. The unequal distribution of boundary

conditions among the tests becomes even more significant when the data is divided into subgroups based on geometric characteristics (i.e., box, in-line, and side-by-side).

Determining the actual degree of fixity under which test piles are loaded is probably a more significant issue than ascertaining the effect that pile-head fixity has on the value of  $G_e$ . To determine  $G_e$  by direct comparison, the boundary condition for the piles in the group should be the same as the single pile boundary condition. If this is not the case, than  $G_e$  may be evaluated inaccurately. For free-headed piles, this determination is not difficult. However, it is very difficult to achieve completely fixed-head conditions for single piles and pile groups. As discussed subsequently in the section on p-multipliers, there are other approaches available for determining  $G_e$  that can be used if the boundary conditions of the group do not match those of the single pile. However, for these methods to yield accurate results, the boundary conditions must be known.

#### *Soil Type and Density*

Sixty-six percent of the tests described in Table 2.4 were performed in sand, 27 % in clay, and 7 % in silt. The results are plotted in Figure 2.10 as a function of soil type, for piles in box arrangements. There does not appear to be any significant trends in this data, except possibly for the tests performed in silty soil. These tests were performed by Prakash and Saran (1967) and appear to yield slightly lower  $G_e$  values than tests performed in clay or sand, at comparable spacings. However, because these were the only tests performed using silty soil and the points are not far below the design line, it seems reasonable to use the same design lines for piles in silt.

The following three studies provide useful information pertaining to the sensitivity of  $G_e$  to soil type or soil density.

- 1.) McVay et al. (1995) performed centrifuge tests on pile groups embedded in loose and medium dense sand at 3D and 5D spacings. From these studies, they

concluded that group efficiency is independent of soil density.

- 2.) Two separate studies were performed on the same 3 by 3 pile group at a site in Texas. The first series of tests were performed with the piles embedded in native clayey soils, and a  $G_e$  of 0.75 was determined (Brown and Reese 1985). The second series of tests were performed after the native soils were replaced with compacted sand. The  $G_e$  determined in this case was 0.77, almost exactly the same as for piles in clay. Thus, changing the soil type from a stiff clay to a medium dense sand had essentially no effect on the measured  $G_e$ .
- 3.) Brown and Shie (1991) investigated group efficiencies using detailed three-dimensional finite element analyses with two different soil models, Von Mises for saturated clay and extended Drucker-Prager for sand. They concluded that the variation in group efficiencies between the two models was too small to warrant consideration in design.

In general, it appears that soil type and soil density do not significantly affect pile group efficiencies.

### ***Pile Displacement***

Group efficiency as defined in Equation 2.11 is independent of pile displacement. It remains to be determined, however, whether  $G_e$  varies with pile displacement, all other things being equal. To gain insight into this question, results from six of the studies described in Table 2.4 were used to calculate values of group efficiency for a range of

pile displacements. The results of these calculations are plotted in Figure 2.11. Based on these plots, it appears that  $G_e$  first decreases as displacement increases, and then becomes constant at deflections in excess of 0.05D (5 % of the pile diameter). The small variations in  $G_e$  at deflections greater than 0.05D fall within the typical range of experimental data scatter, and are insignificant with respect to practical design considerations.

The proposed design curves presented in Figures 2.5 through 2.10 were computed using data for deflections greater than 0.05D. Based on the review of available literature, this appears reasonable, and will yield conservative results for deflections less than 0.05D.

The writer believes that the design curves presented in this section, which are based on the compilation of experimental evidence in Table 2.4, represent the best and most complete values of  $G_e$  that can be currently established. They are recommended as state-of-the-art values for use in analysis and design of laterally loaded pile groups.

## **2.6 P-MULTIPLIERS**

### **2.6.1 Background**

Measurements of displacements and stresses in full-scale and model pile groups indicate that piles in a group carry unequal lateral loads, depending on their location within the group and the spacing between piles. This unequal distribution of load among piles is caused by “shadowing”, which is a term used to describe the overlap of shear zones and consequent reduction of soil resistance. A popular method to account for shadowing is to incorporate p-multipliers into the p-y method of analysis. The p-multiplier values depend on pile position within the group and pile spacing. This section summarizes the current state of knowledge pertaining to p-multipliers, and presents recommendations based on a compilation of available research data.

The concept of  $p$ -multipliers (also called  $f_m$ ) were described by Brown et al. (1988) as a way of accounting for pile group effects by making adjustments to  $p$ - $y$  curves. The multipliers are empirical reduction factors that are experimentally derived from load tests on pile groups. Because they are determined experimentally, the multipliers include both elasticity and shadowing effects. This eliminates the need for a separate  $y$ -multiplier, which is found in many elasticity-based methods. The procedure follows the same approach used in the  $p$ - $y$  method of analysis, except that a multiplier, with a value less than one, is applied to the  $p$ -values of the single pile  $p$ - $y$  curve. This reduces the ultimate soil resistance and softens the shape of the  $p$ - $y$  curve, as shown in Figure 2.2 (b).

Table 2.5 summarizes the results from 11 experimental studies, which present  $p$ -multipliers for pile groups of different sizes and spacings. In these studies, which include 29 separate tests,  $p$ -multipliers were determined through a series of back-calculations using results from instrumented pile-group and single pile load tests. The general procedure for calculating multipliers from load tests results is summarized below.

**Step 1 – Assemble load test data.** Data is required from lateral load tests performed on groups of closely spaced piles and a comparable single pile. At a minimum, the instrumentation program should provide enough data to develop load versus deflection curves for each pile in the group and the single pile. Ideally, the piles will be fully instrumented so that deflections are measured at the top of each pile and strains caused by bending and deformation are measured throughout the length of the piles.

**Step 2 – Develop and adjust single pile  $p$ - $y$  curves.** The goal of this step is to develop a set of  $p$ - $y$  curves that accurately model the soil conditions at the test site based on the measured load response of the single pile. Trial  $p$ - $y$  curves, determined by any suitable method, are adjusted until a good match is obtained between the calculated and the measured response of the single pile.

**Step 3 – Determine  $f_m$  values.** The multipliers are determined in this step through a trial and error process using the  $p$ - $y$  curves developed for the single pile and the measured load versus deflection responses for piles in the group. Trial values of  $f_m$  are adjusted until a good match is obtained between the measured and calculated load versus deflection response curves for each pile.

### 2.6.2 Experimental Studies

Brown and Reese (1985), Morrison and Reese (1986), and McVay et al. (1995) did not detect any significant variation in the response of individual piles within a given row; therefore, they used average response curves for each row of piles rather than attempting to match the response curves for every pile in the group. A similar approach was used by Ruesta and Townsend (1997) and Rollins et al. (1998). In all of these cases, loads were essentially the same for piles in a given row. The current state of practice is thus to use individual row multipliers, rather than separate multipliers for each pile. This approach was followed in all of the studies reported in Table 2.5.

The similarity in behavior between piles in a row is attributed to the pile spacing, which ranged from 3D to 5D in the studies described herein. As discussed in the group efficiency section (see Figure 2.9), side-by-side piles at spacings greater than or equal to 3D are not affected by adjacent piles in the same row. However, at spacings less than 3D, the outer corner piles will take a greater share of load than the interior piles, as demonstrated in Franke's (1988) model tests, and as supported by elasticity-based methods (Poulos 1971b). This implies that corner piles will experience greater bending moments and stresses than interior piles at spacings less than 3D. Ignoring this behavior is unconservative, and could result in overstressed corner piles (in the leading row) for piles spaced at less than 3D.

Franke (1988) performed model tests on 3 side-by-side piles and measured the load that was taken up by each pile. At 3D spacing, the load distribution between the corner piles and center pile was the same. At 2D spacing the corner piles resisted 20 %

more load than the center pile, and at 1D spacing the corner piles resisted 60 % more load.

The generally accepted approach is to assumed that  $p$ -multipliers are constant with depth. That is, a constant  $p$ -multiplier is applied to the set of  $p$ - $y$  curves for all depths in a given pile row. Thus, individual  $p$ - $y$  curves for a pile are adjusted by the same amount, regardless of variations in the soil profile or depth below the ground surface.

The suitability of this assumption was investigated by Brown et al. (1988) during large-scale tests performed on fully instrumented piles. They reported back-calculated  $f_m$  values along the length of three piles, one from each row of the group. As shown in Figure 2.12, variation of  $f_m$  was small and had no affect on the calculated response curve. In reality, the  $p$ - $y$  modifier approach uses an average multiplier that is determined by back-calculating an overall response curve. The modifier is adjusted until the calculated response curve matches the measured response curve. Thus, assuming a constant value of  $f_m$  with depth is reasonable, because the variation of  $f_m$  is implicitly accounted for during the back-calculation procedure.

The test results summarized in Table 2.5 clearly show that the lateral capacity of a pile in a group is most significantly affected by its row position (leading row, first trailing row, etc.) and the center to center pile spacing. The leading row carries more load than subsequent rows; consequently, it has the highest multiplier. Multipliers experimentally measured in these studies are plotted in Figures 2.13 and 2.14 as a function of pile spacing. Figure 2.13 (a) contains data for the leading row, Figure 2.13 (b) the first trailing row, Figure 2.14 (a) the second trailing row, and Figure 2.14 (b) the third and subsequent trailing rows.

Conservative design curves were fitted to the data points using engineering judgement. The four  $f_m$  curves are plotted together in Figure 2.15, which is presented as a proposed design aid. Tests by McVay et al, (1997) indicate that  $f_m$  is essentially the

same for the third, fourth, and subsequent trailing rows. Thus, it appears reasonable to use the 3<sup>rd</sup> trailing row multiplier for the 4<sup>th</sup> pile row and all subsequent rows.

The bending moments computed for the corner piles should be increased if the spacing normal to the direction of load (side-by-side spacing) is less than 3D. Based on the load distributions that were measured by Franke (1988), the bending moments computed using the p-multipliers presented in Figure 2.15 should be adjusted as follows for the corner piles:

<u>side-by-side spacing</u>	<u>corner pile moment modification factor</u>
3D	1.0
2D	1.2
1D	1.6

### 2.6.3 Relationship Between $f_m$ and $G_e$

The overall pile group efficiency,  $G_e$ , can be calculated if the p-multipliers for each row are known, as shown by Equation 2.12.

$$G_e = \frac{\sum_{i=1}^N f_{mi}}{N} \quad \text{Equation 2.12}$$

Where  $N$  is the number of rows in the direction of load and  $f_{mi}$  is the p-multiplier for row  $i$ . Equation 2.12 was used to calculate group efficiencies for seven of the studies reported in Table 2.5. For the purpose of this discussion, the approach used in Equation 2.11 is designated Method A and the approach represented by Equation 2.12 is designated Method B. Group efficiencies calculated using Method A and Method B are plotted together in Figure 2.16, along with the proposed design curve. Method A data points are shown as open squares and Method B points are shown as solid squares.



Group efficiencies calculated using the two different equations should theoretically be the same, and it can be seen that the two approaches yield similar results. However, there can be some discrepancy when results obtained from the two equations are compared. Discrepancies can arise as a result of inconsistencies in matching the single pile and the pile group boundary conditions.

When Method A (Equation 2.11) is used, a direct comparison is made between the resistance of a single pile and the resistance of a pile within the group at a given deflection. However, a direct comparison is not valid unless the pile-head fixity conditions of the single pile are identical to those of the group pile. This is practically impossible. Thus, either analytical adjustments are incorporated into the evaluation, or the difference is simply ignored. If analytical adjustments are used, an estimate of the degree of fixity of both the single pile and group pile is required.

A similar type of judgement regarding pile-head fixity is required for Method B, where  $G_e$  is determined from Equation 2.12. The pile-head boundary condition of the single pile must be estimated when the initial single pile p-y curve is developed. Likewise, pile-head boundary conditions for the group pile must be assumed when  $f_m$  is evaluated during the back-calculation procedure. One way to reduce the uncertainties of these assumptions is to develop the initial set of p-y curves by testing a free-headed single pile, because the free-headed single pile boundary condition is not difficult to obtain in the field. Values of  $f_m$  can then be determined for either a pinned- or fixed-headed group by applying the appropriate boundary conditions during the back-calculation step of the procedure.

The design curves (or design lines, since a linear approximation was assumed) in Figures 2.5, 2.6, 2.7, 2.8, 2.9, 2.10, 2.13, and 2.14 are considered suitable for all except the largest projects, where lateral load behavior of pile groups is an extremely critical issue. For projects where the expense can be justified, these curves can be verified or improved by performing on-site full-scale load tests on groups of instrumented piles.

## 2.7 PILE GROUP BEHAVIOR – ANALYTICAL STUDIES

### 2.7.1 Background

Single pile analytical techniques are not sufficient in themselves to analyze piles within a closely spaced group because of pile-soil-pile interactions and shadowing effects. Numerous methods have been proposed over the last 30 years for evaluating the lateral resistance of piles within a closely spaced group. Table A.2 (Appendix A) summarizes many of these methods, which are classified under four categories, as:

1. closed-form analytical approaches,
2. elasticity methods,
3. hybrid methods, and
4. finite element methods.

Pertinent features of these approaches are described in the following paragraphs.

### 2.7.2 Closed-Form Analytical Approaches

Many of the methods in this category combine empirical modifying factors with single-pile analytical techniques. The oldest techniques simply involve applying a group efficiency factor to the coefficient of subgrade reaction. Kim (1969) used this approach to model the soil and replaced the pile with an equivalent cantilever beam. Bogard and Matlock (1983) used a group efficiency factor to soften the soil response and modeled the pile group as an equivalent large pile. This method is similar to the  $p$ -multiplier approach, which was described in the Section 2.6.

### 2.7.3 Elasticity Methods

Methods that fall into this category model the soil around the piles as a three-dimensional, linearly elastic continuum. Mindlin's equations for a homogenous,

isotropic, semi-infinite solid are used to calculate deformations. This is similar to the single pile approach except elastic interaction factors are incorporated into the analyses. These factors are used to address the added displacements and rotations of a pile within a group caused by movements of adjacent piles.

In the original approach used by Poulos (1971b), the expression for single pile deflection, Equation 2.10, was modified for pile-soil-pile interaction effects by including the influence factors,  $\mathbf{a}_r$  and  $\mathbf{a}_q$ , to account for the additional horizontal displacements and rotations of pile  $i$  caused by displacement of pile  $j$ . These factors were defined as follows:

$$\mathbf{a}_r = \frac{\text{additional displacement caused by adjacent pile}}{\text{displacement of pile caused by its own loading}}$$

$$\mathbf{a}_q = \frac{\text{additional rotation caused by adjacent pile}}{\text{rotation of pile caused by its own loading}}$$

Poulos and Davis (1980) present the interaction factors in chart form for various conditions. The displacement and rotations of any pile in the group is obtained using the principle of superposition. This implies that the increase in displacement of a pile due to all the surrounding piles can be calculated by summing the increases in displacement due to each pile in turn using interaction factors (Poulos 1971b).

Using the principle of superposition, the displacement of a pile within a group,  $y_k$ , is determined by modifying the single pile equation (Equation 2.10) using the interaction factors and the principle of superposition. The deflection of pile  $k$ , within a group is given by:

$$y_k = y_s \left[ \sum_{j=1}^n (p_j \mathbf{a}_{kj}) + p_k \right] \quad \text{Equation 2.13}$$

where  $y_s$  is the displacement of a single pile,  $p_j$  is the load on pile  $j$ ,  $a_{kj}$  is the interaction factor corresponding to the spacing and angle between piles  $k$  and  $j$ ,  $n$  is the number of piles in the group, and  $p_k$  is the load on pile  $k$ .

The total load on the group,  $p_g$ , is determined by superposition as:

$$p_g = \sum_{j=1}^n p_j \quad \text{Equation 2.14}$$

In addition to Poulos's chart solutions, there are a number of computer programs available including: PIGLET, DEFPIG, and PILGPI (Poulos 1989).

Other elastic continuum methods are available that use numerical techniques in place of Mindlin's equations. These include the boundary element method (Banerjee and Davies, 1978 and 1979), algebraic equations fitted to finite element results (Randolph 1981), numerical procedures (Iyer and Sam 1991), semi-empirical methods using radial strain components (Clemente and Sayed 1991), and finite element methods (discussed under a separate heading).

#### 2.7.4 Hybrid Methods

These methods are called hybrid because they combine the nonlinear  $p$ - $y$  method with the elastic continuum approach.  $p$ - $y$  curves are used to model the component of soil deflection that occurs close to individual piles (shadow effect) and elastic continuum methods are used to approximate the effects of pile-soil interaction in the less highly stressed soil further from the piles. Focht and Koch (1973) developed the original hybrid procedure in which elasticity-based  $\alpha$ -factors are used in conjunction with  $y$ -multipliers. Reese et al. (1984) modified the Focht-Koch approach by using solutions from  $p$ - $y$  analyses to estimate elastic deflections where load-deflection behavior is linear. O'Neill et al. (1977) modified the Focht-Koch approach by adjusting unit-load transfer curves individually to account for stresses induced by adjacent piles. Additional hybrid

approaches include Garassino's (1994) iterative elasticity method and Ooi and Duncan's (1994) group amplification procedure.

### 2.7.5 Finite Element Methods

Finite element approaches typically model the soil as a continuum. Pile displacements and stresses are evaluated by solving the classic beam bending equation (Equation 2.3) using one of the standard numerical methods such as Galerkin (Iyer and Sam 1991), collocation, or Rayleigh-Ritz (Kishida and Nakai 1977). Various types of elements are used to represent the different structural components. For instance, the computer program Florida Pier (McVay et al. 1996) uses three-dimensional two-node beam elements to model the piles, pier columns, and pier cap, and three-dimensional 9-node flat shell elements for the pile cap. Interface elements are often used to model the soil-pile interface. These elements provide for frictional behavior when there is contact between pile and soil, and do not allow transmittal of forces across the interface when the pile is separated from the soil (Brown and Shie 1991).

Another finite element computer program that has been used to analyze pile groups is the computer program GPILE-3D by Kimura et al. (1995). Kimura and his co-workers initially used column elements in the computer program to represent the piles. They later discovered that column elements alone were not sufficient to adequately model the response of pile groups; thus, subsequent modifications were made to their computer code to model the piles with both beam and column elements. They found that using this combination of elements with the Cholesky resolution method allowed them to better simulate the load-displacement relationship of a nonlinear pile in a 3-D analysis.

The soil stress-strain relationship incorporated into the finite element model is one of the primary items that delineate the various finite element approaches. This relationship may consist of a relatively straightforward approach using the subgrade reaction concept with constant or linearly varying moduli, or a complex variation of the elastic continuum method. For instance, Sogge's (1984) one-dimensional approach

models the soil as a discrete series of springs with a stiffness equivalent to the modulus of subgrade reaction. Sogge used the modulus of subgrade reaction, as defined in Equation 2.5, to develop  $p$ - $y$  curves for input into the computer model.

Desai et al. (1980) used a much more rigorous approach to calculate the soil modulus in their two-dimensional approach. They calculated nonlinear  $p$ - $y$  curves using the tangent modulus,  $E_{st}$ , obtained from a modified form of the Ramberg-Osgood model. Brown and Shie (1991) performed a three-dimensional study using a simple elastic-plastic constant yield strength envelope (Von Mises surface) to model a saturated clay soil and a modified Drucker-Prager model with a nonassociated flow rule for sands.

Adachi et al. (1994) performed a 3-D elasto-plastic analysis using a Drucker-Prager yield surface for the soil and a nonlinear model (trilinear curve) for the concrete piles, which accounted for the decrease in bending rigidity and cracking at higher loads. The pile response was modeled using a bending moment versus pile curvature relationship with three points of deflection, defined as: (1) the initial cracking point of the concrete, (2) the yield point of the reinforcing steel, and (3) the ultimate concrete capacity. A hyperbolic equation was fit to the three points to obtain a smooth curve for the computer analysis.

The current trend in finite element analyses is the development of more user-friendly programs such as Florida Pier (Hoit et al. 1997). The developers of these programs have attempted to overcome some of the difficulties that practicing engineers have with the finite element method by incorporating interactive graphical pre- and post-processors. For instance, in Florida Pier the finite element mesh is internally created in the pre-processor based on the problem geometry. Florida Pier's post-processor displays the undeflected and deflected shape of the structure, along with internal forces, stresses, and moments in the piles and pier columns.

## **2.8 SUMMARY**

A comprehensive literature review was conducted to examine the current state of knowledge regarding pile cap resistance and pile group behavior. Over 350 journal articles and other publications pertaining to lateral resistance, testing, and analysis of pile caps, piles, and pile groups were collected and reviewed. Pertinent details from these studies were evaluated and, whenever possible, assimilated into tables and charts so that useful trends and similarities can readily be observed.

Of the publications reviewed, only four papers were found that described load tests performed to investigate the lateral resistance of pile caps. These studies indicate that the lateral resistance of pile caps can be quite significant, especially when the cap is embedded beneath the ground surface.

A review of the most widely recognized techniques for analyzing laterally loaded single piles was provided. These techniques provide a framework for methods that are used to evaluate the response of closely spaced piles, or pile groups. Modifications of single pile techniques are often in the form of empirically or theoretically derived factors that are applied, in various ways, to account for group interaction effects.

Piles in closely spaced groups behave differently than single isolated piles because of pile-soil-pile interactions that take place in the group. Deflections and bending moments of piles in closely spaced groups are greater than deflections and bending moments of single piles, at the same load per pile, because of these interaction effects.

The current state of practice regarding pile group behavior was reviewed from an experimental and analytical basis. Thirty-seven experimental studies were reviewed in which the effects of pile group behavior were observed and measured. These included 15 full-scale field tests, 16 1g model tests, and 6 geotechnical centrifuge tests. Approximately 30 analytical studies were reviewed that addressed pile group lateral

behavior. These studies included closed-form analytical approaches, elasticity methods, hybrid methods, and finite element methods.

Based on these studies, the following factors were evaluated to determine their influence on pile group behavior, and more specifically, pile group efficiency ( $G_e$ ).

1. **Pile spacing.** Pile spacing is the most dominant factor affecting pile group behavior. Group effects are negligible when center to center pile spacing exceeds 6 pile diameters (6D) in the direction of load and when they exceed 3D measured in a direction normal to load. The efficiency of a pile group decreases as pile spacings drop below these values.
2. **Group arrangement.** After pile spacing, the next most significant factor appears to be the geometric arrangement of piles within the group. Group efficiencies were evaluated for the three most common geometric arrangements used in practice, which are defined in Figure 2.3 as: box arrangement, in-line arrangement, and side-by-side arrangement.
3. **Group Size.** The effect of group size on piles in box arrangements or side-by-side arrangements could not be discerned from the data available. Sufficient data was available to evaluate the influence of group size on in-line arrangements of piles, as shown in Figure 2.7. At a given spacing, the group efficiency decreases as the number of piles in a line increase.
4. **Pile head fixity.** Significant conclusions regarding the impact of pile head restraint on group efficiency were not possible because of limited experimental data. However, quantifying the actual degree of fixity under which test piles are loaded is probably a more significant issue than ascertaining the effect that pile-head fixity has on the value of group efficiency.



5. **Soil type and density.** Based on the evaluation of 37 experimental studies in different soils, there is no significant relationship between soil type or density and group efficiency.
6. **Pile displacement.** The influence of pile displacement on group efficiency ( $G_e$ ) was evaluated using the results from six experimental studies. As shown in Figure 2.11,  $G_e$  first decreases as displacement increases, and then becomes constant at deflections in excess of 0.05D (5 % of the pile diameter). The small variations in  $G_e$  at deflections greater than 0.05D fall within the typical range of experimental data scatter, and are insignificant with respect to practical design considerations.

Measurements of displacements and stresses in full-scale and model pile groups indicate that piles in a group carry unequal lateral loads, depending on their location within the group and the spacing between piles. This unequal distribution of load among piles is caused by “shadowing”, which is a term used to describe the overlap of shear zones and consequent reduction of soil resistance. A popular method to account for shadowing is to incorporate p-multipliers ( $f_m$ ) into the p-y method of analysis. The p-multiplier values depend on pile position within the group and pile spacing. The multipliers are empirical reduction factors that are experimentally derived from load tests on pile groups. Because they are determined experimentally, the multipliers include both elasticity and shadowing effects.

The results from 11 experimental studies were reviewed in which p-multipliers for pile groups of different sizes and spacings were developed. In these studies, which include 29 separate tests, p-multipliers were determined through a series of back-calculations using results from instrumented pile-groups and single pile load tests.

Multipliers applied to p-y curves and group efficiency factors represent two approaches for quantifying group interaction effects. Because these approaches theoretically represent the same phenomenon, the factors summarized above for

empirically derived  $G_e$  values apply equally as well to the empirically derived  $f_m$  values. Three additional factors that are more specific to p-multipliers are summarized below:

1. **Depth.** The p-y modifier approach uses an average multiplier that is determined by back-calculating an overall response curve. The modifier is adjusted until the calculated response curve matches the measured response curve. Thus, assuming a constant value of  $f_m$  with depth is reasonable, because the variation of  $f_m$  is implicitly accounted for during the back-calculation procedure.
2. **Row position.** The lateral capacity of a pile in a group is significantly affected by its row position (leading row, first trailing row, etc.) and the center to center pile spacing. The leading row carries more load than subsequent rows; consequently, it has the highest multiplier. Multipliers decrease going from the leading to the trailing row, which has the lowest multiplier.
3. **Corner pile effects.** At spacings less than 3D, the outer corner piles will take a greater share of load than interior piles, and consequently, will experience greater bending moments and stresses. Ignoring this behavior is unconservative, and could result in overstressed corner piles. Recommendations were presented for modifying bending moments computed for the corner piles if the spacing normal to the direction of load (side-by-side spacing) is less than 3D.

Design lines were developed for estimating pile group efficiency values and p-multipliers as functions of pile arrangement and pile spacing. To the extent possible, the lines account for the factors described above. The design lines are presented in chart form, as follows:

- Group efficiency versus pile spacing for piles in a box arrangement – Figure 2.5.

- Group efficiency versus pile spacing for piles oriented in-line – Figure 2.7.
- Group efficiency versus pile spacing for piles oriented side-by-side – Figure 2.9.
- p-multipliers for the leading row, 1<sup>st</sup> trailing row, 2<sup>nd</sup> trailing row, and 3<sup>rd</sup> and subsequent trailing rows – Figure 2.15.

These design lines represent state-of-the-art values for use in analysis and design of laterally loaded pile groups. The writer believes that these lines are suitable for all except the largest projects, where lateral load behavior of pile groups is an extremely critical issue. For projects where the expense can be justified, these lines can be verified or improved by performing full-scale load tests on groups of instrumented piles.

Table 2.1. Summary of previous load tests performed to evaluate the lateral resistance of pile caps.

Reference	Pile Type	Cap Size	Foundation Soils	Cap Contribution*
Beatty 1970	2 x 3 group of step-tapered mandrel driven concrete piles	not reported	miscellaneous fill over soft silty clay and clay	more than 50%
Kim and Singh 1974	2 x 3 group of 10BP42 steel piles	12' long x 8' wide x 4' thick	silty and sandy clay, with $S_{uavg} \approx 1$ tsf in top 15'	about 50%
Rollins et al. 1997	3 x 3 group of 12" dia. steel pipe piles	9' long x 9' wide x 4' thick	compacted sandy gravel fill over silt and clay	about 50%
Zafir and Vanderpool 1998	2 x 2 group of 2' dia. drilled shafts	11' diameter by 10' thick	silty sand, clayey sand, and sandy clay with caliche layers	more than 50%

\* "Cap Contribution" reflects the approximate contribution of the pile cap to the lateral load resistance of the pile group at a given lateral deflection.

Table 2.2 Summary of full-scale field test details.

<b>Pile Type</b>	<b>Installation Method</b>	<b>Soil Type</b>	<b>Pile Head Boundary Condition</b>
steel – 9	driven – 13	sand – 8	fixed-head – 6
concrete – 4	bored - 3	clay - 6	free-head – 5
timber - 4	–	not reported - 1	pinned-head - 5

Table 2.3 Geotechnical centrifuge facility details.

<b>Reference</b>	<b>Facility Location</b>	<b>Approx. Arm Radius (ft)</b>	<b>Test Acceleration (gravity)</b>	<b>Container Capacity (ft<sup>3</sup>)</b>
Barton (1984)	Cambridge, England	13	30g to 120g	8
Zhang and Hu (1991)	S.W. Institute of Mechanics, China	35	50g	not reported
Adachi et al. (1994)	Kyoto University, Japan	8	40g	2
McVay et al. (1994, 1995, 1998)	University of Florida, USA	5	45g	1.25

Table 2.4. Summary of pile group efficiency test data.

Reference	Group arrangement	Group size	c/c pile spacing	$G_e$	Type of test	Pile type	Soil	Deflection (dia.)
Prakash and Saran (1967)	box	2x2	3D	0.48	1g model fixed-head	0.355 in dia. aluminum tube	silt (ML) strength not reported	0.11D
		2x2	4D	0.66				
		2x2	5D	0.78				
		3x3	3D	0.49				
		3x3	4D	0.59				
		3x3	5D	0.63				
Cox et al. (1984)	in-line	1x3	1.5D	0.59	1g model free-head	1.0 in dia. steel tube	v. soft clay $S_u = .042$ ksf	0.2D
		1x3	2D	0.70				
		1x3	3D	0.81				
		1x3	4D	0.86				
		1x3	6D	0.95				
		1x5	1.5D	0.54				
		1x5	2D	0.59				
		1x5	3D	0.78				
Cox et al. (1984)	side-by-side	3x1	1.5D	0.76	1g model free-head	2.0 in dia. steel tube	v. soft clay $S_u = .042$ ksf	0.2D
		3x1	2D	0.85				
		3x1	4D	0.99				
		5x1	1.5D	0.80				
		5x1	2D	0.85				
		5x1	3D	0.98				
Brown and Reese (1985)	box	3x3	3D	0.75	full scale field free-head	10.75 in dia pipe piles.	stiff OC clay $S_u = 1.2$ to 1.7 ksf	0.05D

Table 2.4. Continued.

Reference	Group arrangement	Group size	c/c pile spacing	$G_e$	Type of test	Pile type	Soil	Deflection (dia.)
Sarsby (1985)	in-line	1x2	2D	0.70	1g model free-head	0.24 in dia. mild steel bars	sand (SP) $\phi = 38^\circ$	extrapo- lated to zero
		1x2	4D	0.78				
		1x2	8D	0.84				
		1x2	12D	0.90				
		1x3	2D	0.66				
		1x3	4D	0.74				
		1x3	8D	0.82				
		1x3	12D	0.84				
		1x4	2D	0.64				
		1x4	4D	0.74				
1x4	8D	0.80						
Morrison and Reese (1986)	box	3x3	3D	0.77	full scale field free-head	10.75 in dia pipe piles.	med. dense sand $D_r = 50\%$ $\phi = 38.5^\circ$	0.05D
Franke (1988)	in-line	1x3	2D	0.60	1g model free-head	0.16 in dia. type not reported	fine sand $D_r$ not reported	not reported
		1x3	3D	0.65				
		1x3	4D	0.80				
		1x3	6D	1.0				
Franke (1988)	side-by-side	3x1	1D	0.74	1g model free-head	0.16 in dia. type not reported	fine sand $D_r$ not reported	not reported
		3x1	2D	0.85				
		3x1	3D	1.0				
		3x1	4D	1.0				

Table 2.4. Continued.

Reference	Group arrangement	Group size	c/c pile spacing	$G_e$	Type of test	Pile type	Soil	Deflection (dia.)
Lieng (1989)	in-line	1x2	2D	0.77	1g model free-head	5.9 in dia. aluminum pipes	dry loose sand $D_r$ not reported	0.03D to 0.05D
		1x2	3D	0.93				
		1x2	4D	0.94				
		1x2	5D	0.99				
Lieng (1989)	side-by-side	2x1	2D	0.92	1g model free-head	5.9 in dia. aluminum pipes	dry loose sand $D_r$ not reported	0.07D to 0.13D
		2x1	3D	1.0				
		2x1	4D	1.0				
Shibata et al. (1989)	in-line	1x2	2D	0.75	1g model free-head	0.87 in dia. aluminum tubes	uniform sand $D_r = 20\%$	0.1D to 0.3D
		1x2	2.5D	0.76				
		1x2	5D	1.0				
Shibata et al. (1989)	side-by-side	4x1	2D	0.62	1g model free-head	0.87 in dia. aluminum tubes	uniform sand $D_r = 20\%$	0.1D to 0.3D
		4x1	2.5D	0.75				
		4x1	5D	1.0				
Shibata et al. (1989)	box	3x3	2D	0.40	1g model free-head	0.87 in dia. aluminum tubes	uniform sand $D_r = 20\%$	0.1D to 0.3D
		3x3	2.5D	0.45				
		3x3	5D	0.70				
		4x4	2D	0.34				
		4x4	2.5D	0.40				
		4x4	5D	0.70				



Table 2.4. Continued.

Reference	Group arrangement	Group size	c/c pile spacing	$G_e$	Type of test	Pile type	Soil	Deflection (dia.)
Shibata et al. (1989)	box	3x3	2D	0.58	1g model free-head	0.87 in dia. chloridized-vinyl tubes	uniform sand $D_r = 20\%$	0.1D to 0.3D
		3x3	2.5D	0.78				
		3x3	5D	1.0				
		4x4	2D	0.43				
		4x4	2.5D	0.60				
		4x4	5D	0.98				
Adachi et al. (1994)	in-line	1x2	2D	0.81	40g centrifuge pinned-head	63 in dia. prototype	v. dense sand $D_r = 90\%$	0.07D to 0.10D
			4D	0.92				
Adachi et al. (1994)	side-by-side	2x1	2D	0.92	40g centrifuge pinned-head	63 in dia. prototype	v. dense sand $D_r = 90\%$	0.07D to 0.10D
Kotthaus et al. (1994)	in-line	1x3	3D	0.70	50g centrifuge fixed-head	59 in dia. prototype	v. dense sand $D_r = 98\%$ $\phi = 38^\circ$	0.10D
		1x3	4D	0.83				
McVay et al. (1994, 1995)	box	3x3	3D	0.73	45g centrifuge free-head	17 in dia. prototype	loose sand $D_r = 33\%$	0.15D
		3x3	5D	0.92				
McVay et al. (1994, 1995)	box	3x3	3D	0.74	45g centrifuge free-head	17 in dia. prototype	med. dense sand $D_r = 55\%$	0.15D
		3x3	5D	0.95				

Table 2.4. Concluded.

Reference	Group arrangement	Group size	c/c pile spacing	$G_e$	Type of test	Pile type	Soil	Deflection (dia.)
Rao et al. (1996)	in-line	1x2	3D	0.78	1g model fixed head	0.85 in dia. mild steel pipes	marine clay (CH) $S_u=1.8$ ksf	0.47D
		1x2	4D	0.96				
		1x2	5D	0.99				
		1x2	6D	1.05				
Rao et al. (1996)	in-line	2x1	3D	0.97	1g model fixed head	0.85 in dia. mild steel pipes	marine clay (CH) $S_u=1.8$ ksf	0.47D
		2x1	4D	0.99				
		2x1	5D	1.0				
Ruesta and Townsend (1997)	box	4x4	3D	0.80	full-scale free-head	30 in square prestressed concrete	loose fine sand $D_r = 30\%$ $\phi = 32^\circ$	0.05D to 0.1D
Rollins et al. (1998)	box	3x3	3D	0.67	full-scale pinned-head	12 in dia. steel pipe	CL-ML and CL $S_u = .5$ to 1.0 ksf	0.065D

Table 2.5. Summary of p-multiplier ( $f_m$ ) test data.

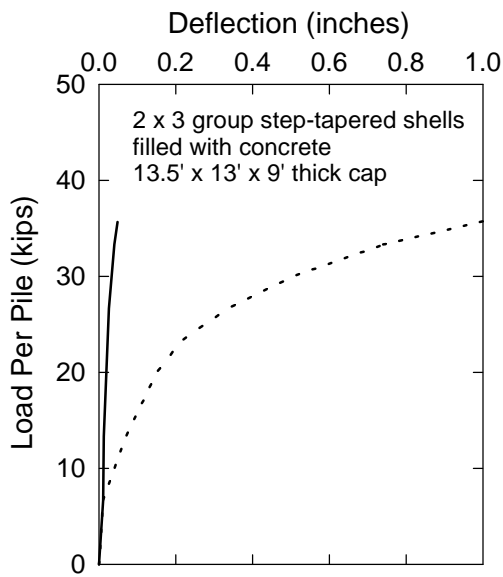
Reference and soil type	Pile size and arrangement	c/c pile spacing (dia.)	Deflection range (diameter)	$G_e$	p-multiplier ( $f_m$ )				
					Leading row	1 <sup>st</sup> trailing row	2 <sup>nd</sup> trailing row	3 <sup>rd</sup> trailing row	4 <sup>th</sup> trailing row
Cox et al. (1984), very soft clay	1 in dia., in-line 1x4 and 1x3	1.5D	0 to 0.25D	0.53	0.77	0.50	0.40	0.47	
		2D		0.59	0.80	0.53	0.55	0.49	
		3D		0.81	0.96	0.77	0.77	0.74	
		4D		0.89	0.97	0.87	0.84	--	
		6D		0.95	1.00	0.92	0.92	--	
Brown and Reese (1985), stiff clay	10.75 in dia., box 3x3	3D	0 to 0.23D	0.60	0.70	0.60	0.50		
Meimon et al. (1986), stiff silty clay	11 in square, 2 piles in-line	3D	0 to 0.1D	0.70	0.90	0.50			
Morrison and Reese (1986), med. dense sand	10.75 in dia., box 3x3	3D	0 to 0.23D	0.50	0.80	0.40	0.30		

Table 2.5. Continued.

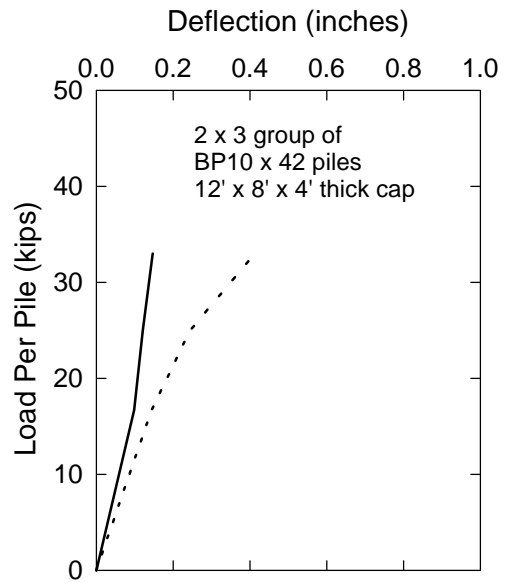
Reference and soil type	Pile size and arrangement	c/c pile spacing (dia.)	Deflection range (diameter)	$G_e$	p-multiplier ( $f_m$ )				
					Leading row	1 <sup>st</sup> trailing row	2 <sup>nd</sup> trailing row	3 <sup>rd</sup> trailing row	4 <sup>th</sup> trailing row
Lieng (1989), loose sand	5.9 in dia., 2 piles in-line	2D 3D 4D 5D 6D	0 to 0.13D	--	not measured	0.33 0.60 0.80 0.93 1.0			
Brown and Shie (1991), computed-FEM, avg. soil	10.75 in dia., 2 piles in-line	2D 3D 5D	0 to 0.14D	-- 0.70 0.90	0.80 0.90 1.0	-- 0.50 0.80			
McVay et al. (1994, 1995), loose sand	16.88 in dia, box. 3x3	3D 5D	0 to 0.14D 0 to 0.20D	0.48 0.85	0.65 1.0	0.45 0.85	0.35 0.70		
McVay et al. (1994, 1995), med. dense sand	16.88 in dia, box. 3x3	3D 5D	0 to 0.16D 0 to 0.19D	0.50 0.85	0.80 1.0	0.40 0.85	0.30 0.70		

Table 2.5. Concluded

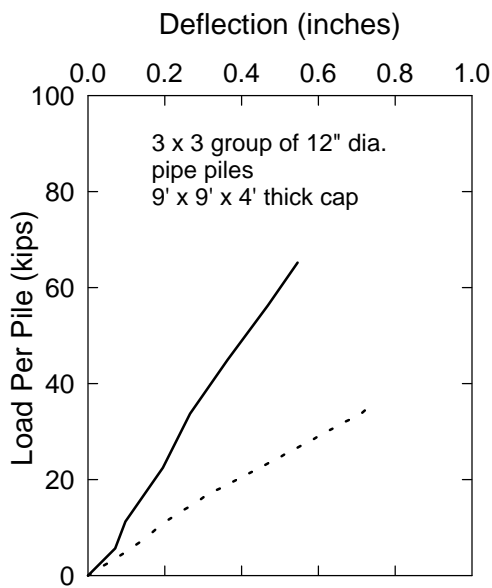
Reference and soil type	Pile size and arrangement	c/c pile spacing (dia.)	Deflection range (diameter)	$G_e$	p-multiplier ( $f_m$ )				
					Leading row	1 <sup>st</sup> trailing row	2 <sup>nd</sup> trailing row	3 <sup>rd</sup> trailing row	4 <sup>th</sup> trailing row
Ruesta and Townsend (1997), loose sand	30 in square, box 4x4	3D	0 to 0.10D	0.53	0.80	0.70	0.30	0.30	
McVay et al. (1998), med. dense sand	16.88 in dia., box 3x3 to 3x7	3D	0 to 0.20D	0.50	0.80	0.40	0.30	--	--
		3D	0 to 0.26D	.045	0.80	0.40	0.30	0.30	--
		3D	0 to 0.27D	0.40	0.80	0.40	0.30	0.20	0.30
		3D	0 to 0.26D	0.38	0.80	0.40	0.30	0.20	0.20
		3D	0 to 0.20D	0.34	0.80	0.40	0.30	0.20	0.20
McVay et al. (1998), continued		3x3	<i>continued from previous row</i>				--	<b>5<sup>th</sup> trailing row</b>	<b>6<sup>th</sup> trailing row</b>
		3x4					--		
		3x5					--		
		3x6					3x6	0.30	--
		3x7					3x7	0.20	0.30
Rollins et al. (1998), clayey silt	12 in dia. box 3x3	3D	0 to 0.19D	0.47	0.60	0.40	0.40		



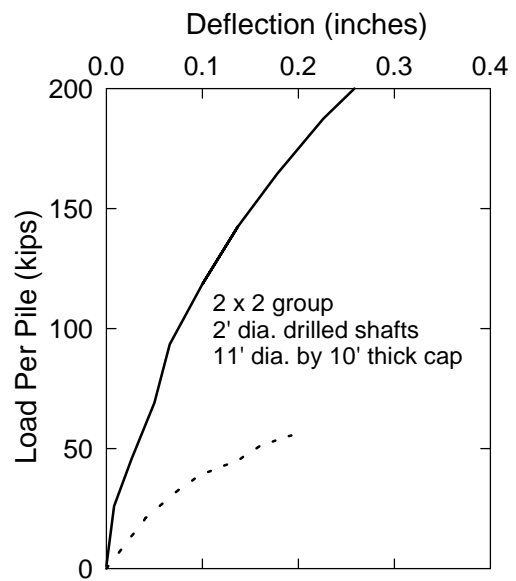
(a) Beatty, 1970.



(b) Kim and Singh, 1974.



(c) Rollins et al., 1997.



(d) Zafir and Vanderpool, 1998.

Legend for all 4 plots

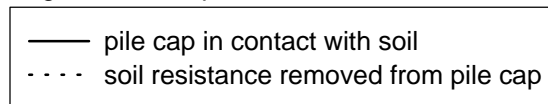
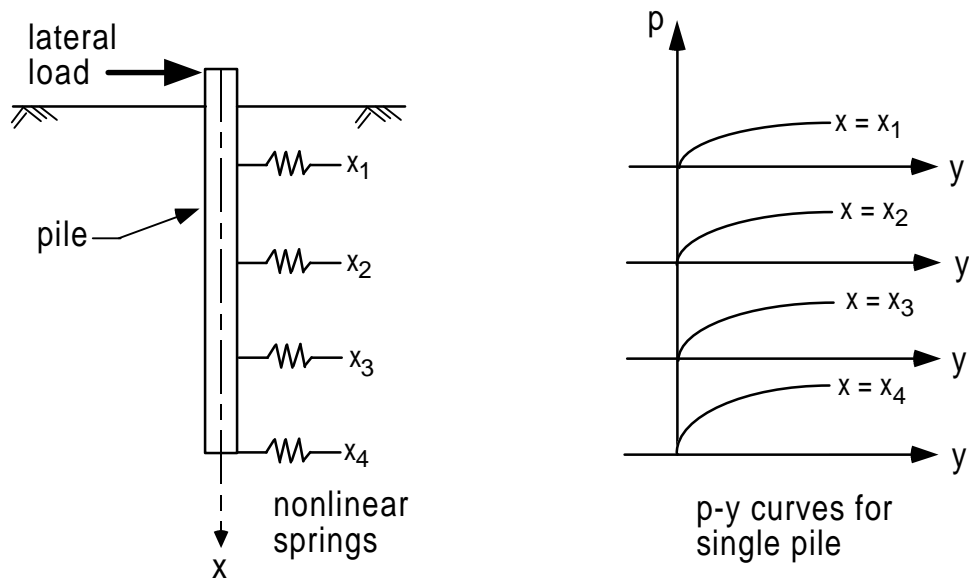
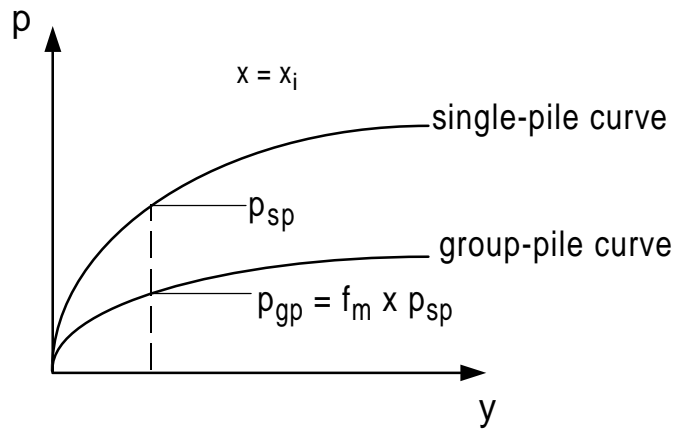


Figure 2.1. Comparison of published load versus deflection curves.

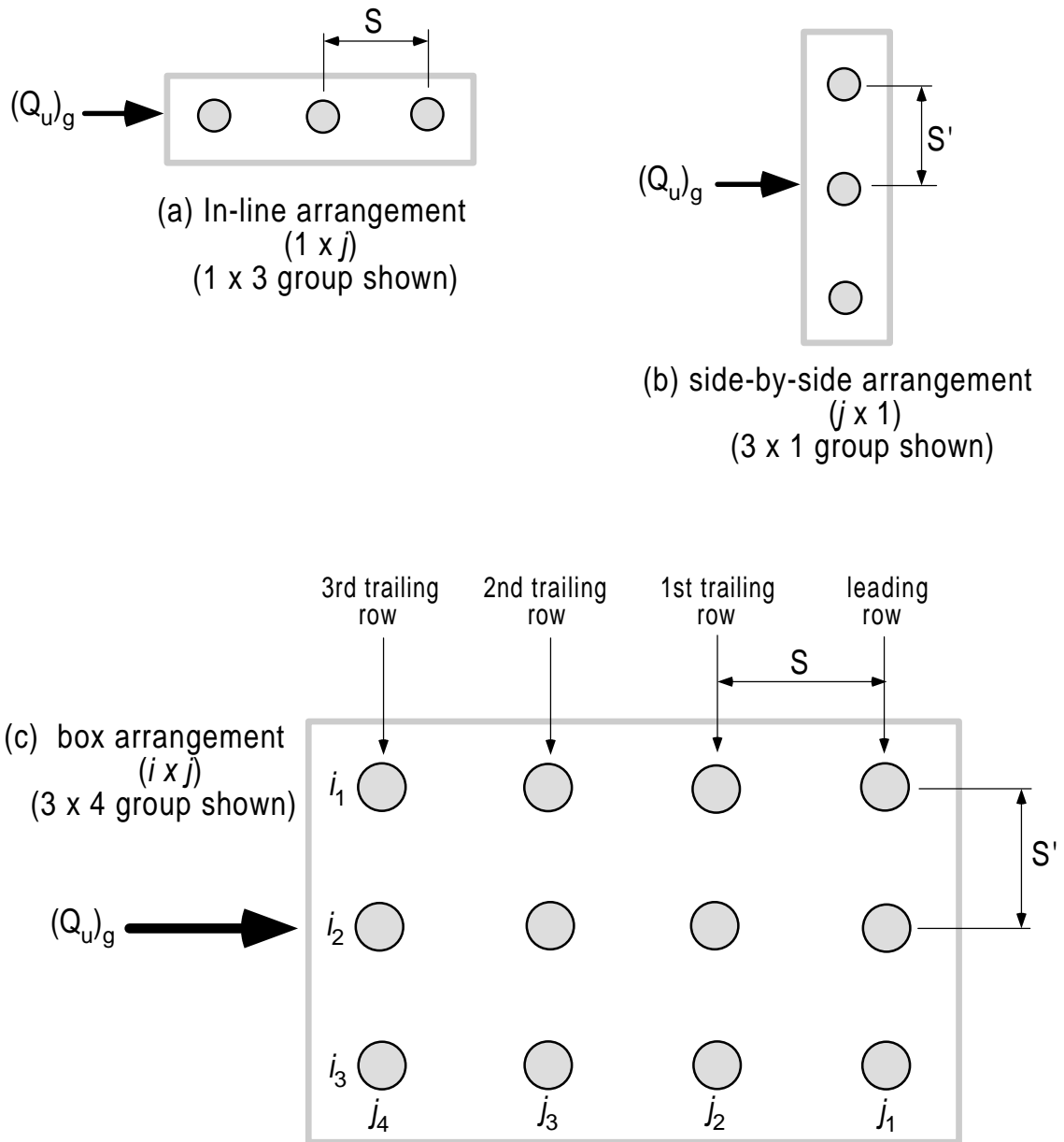


(a) Single pile model.



(b) P-multiplier concept for lateral group analysis.

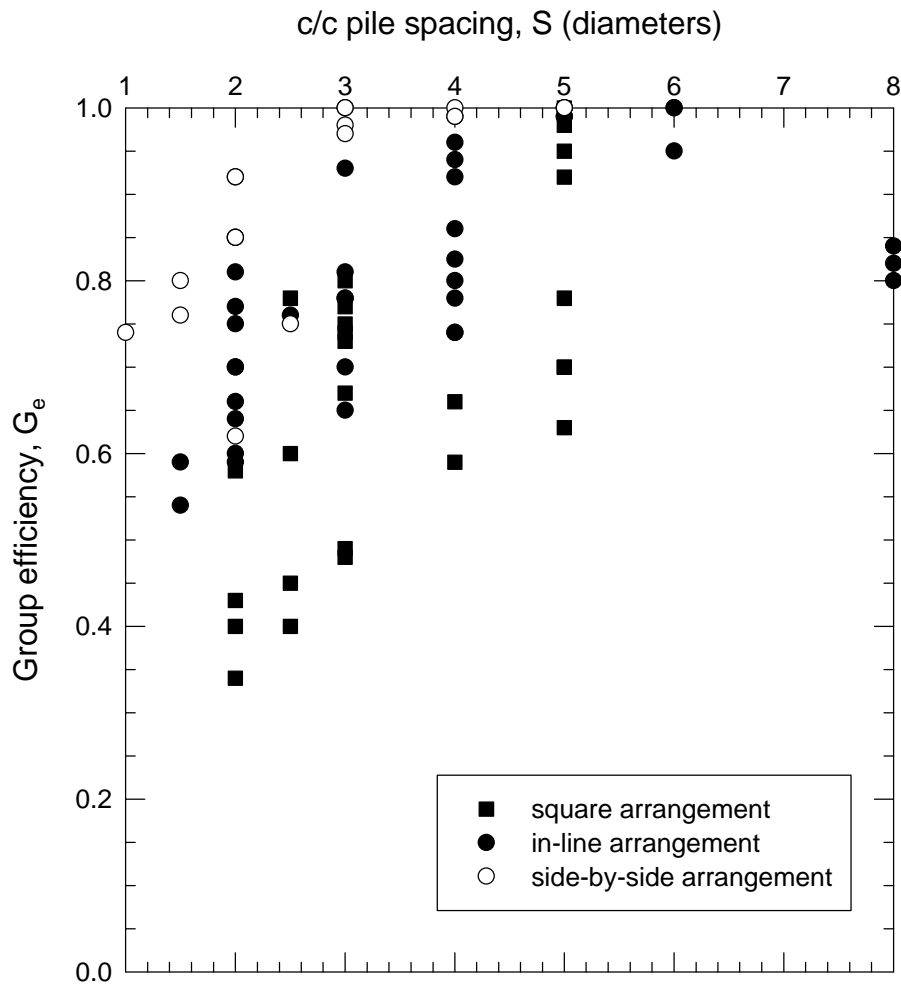
Figure 2.2. p-y Models for laterally loaded piles.



$S$  = c/c spacing in direction of load  
 $S'$  = c/c spacing perpendicular to direction of load  
 $i$  = number of in-line rows  
 $j$  = number of side-by-side rows  
 $(Q_u)_g$  = horizontal load applied to pile group

Figure 2.3. Description of terms used to describe pile group arrangements.





where,  $G_e = \frac{(Q_u)_g}{n(Q_u)_s}$

Figure 2.4. Group efficiency versus pile spacing for all reported pile arrangements (square, in-line, and side-by-side).

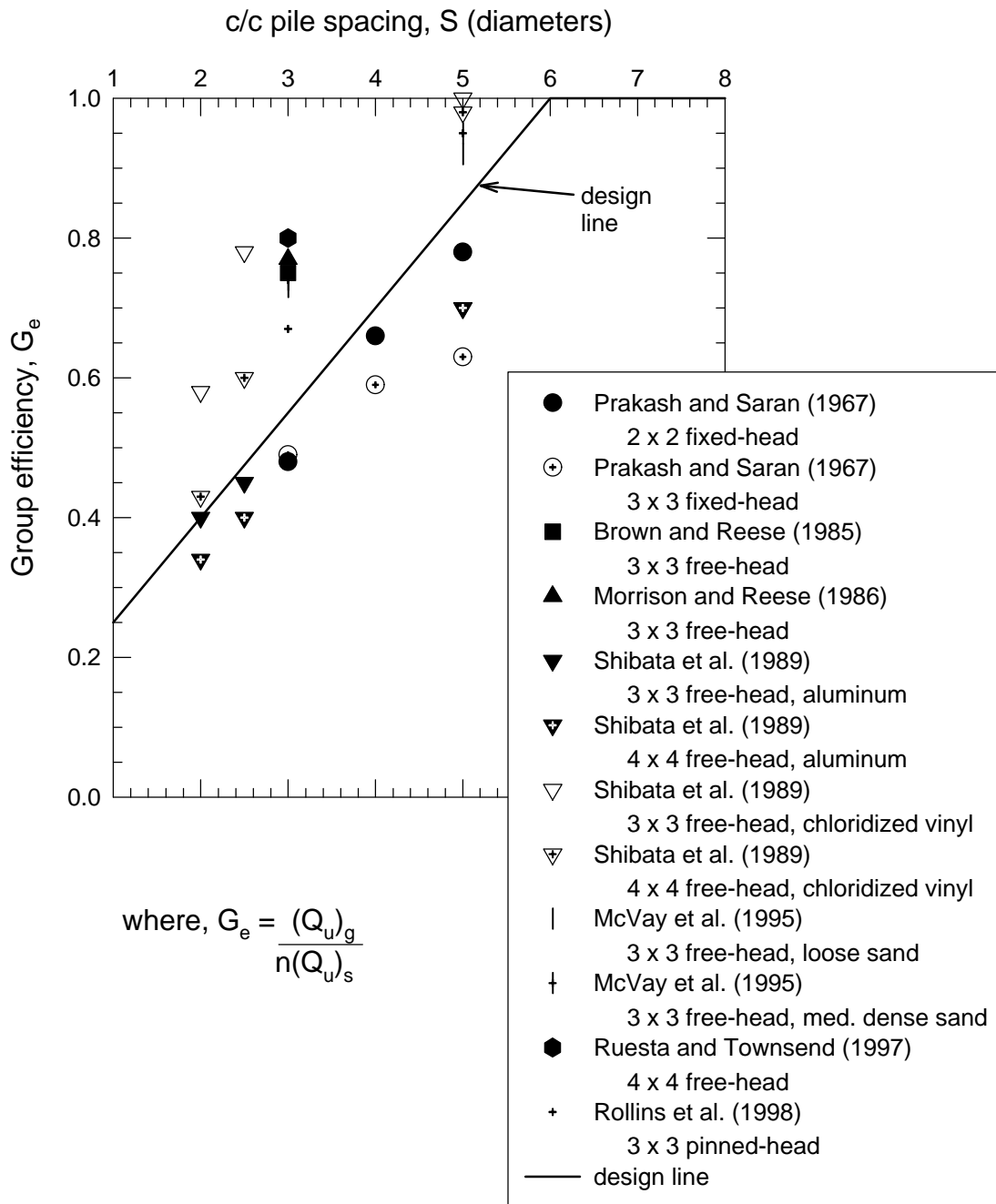
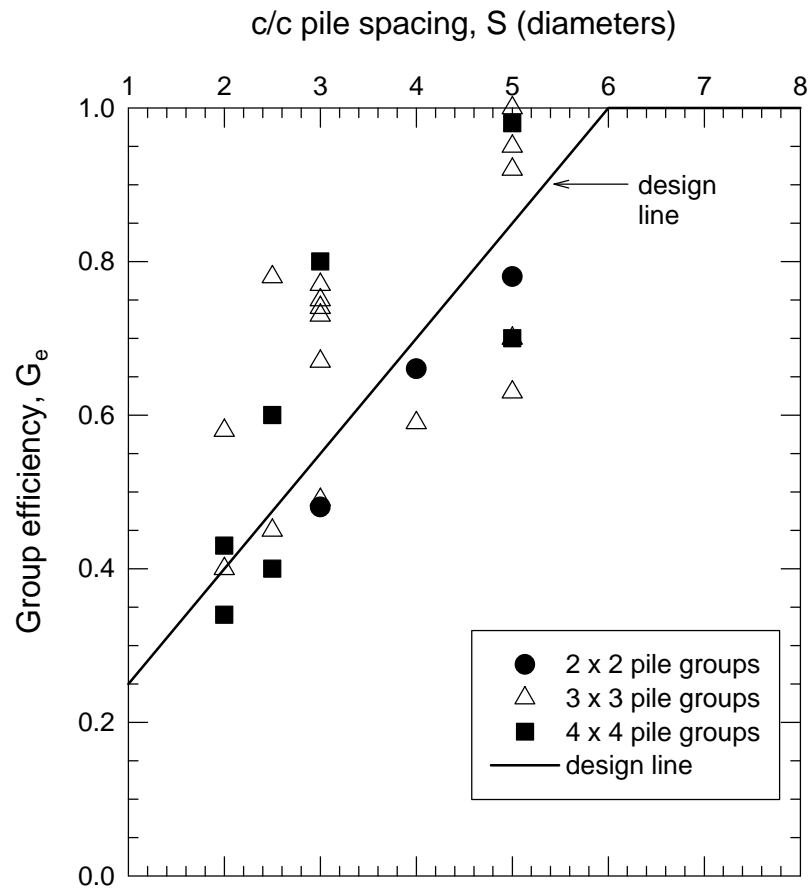
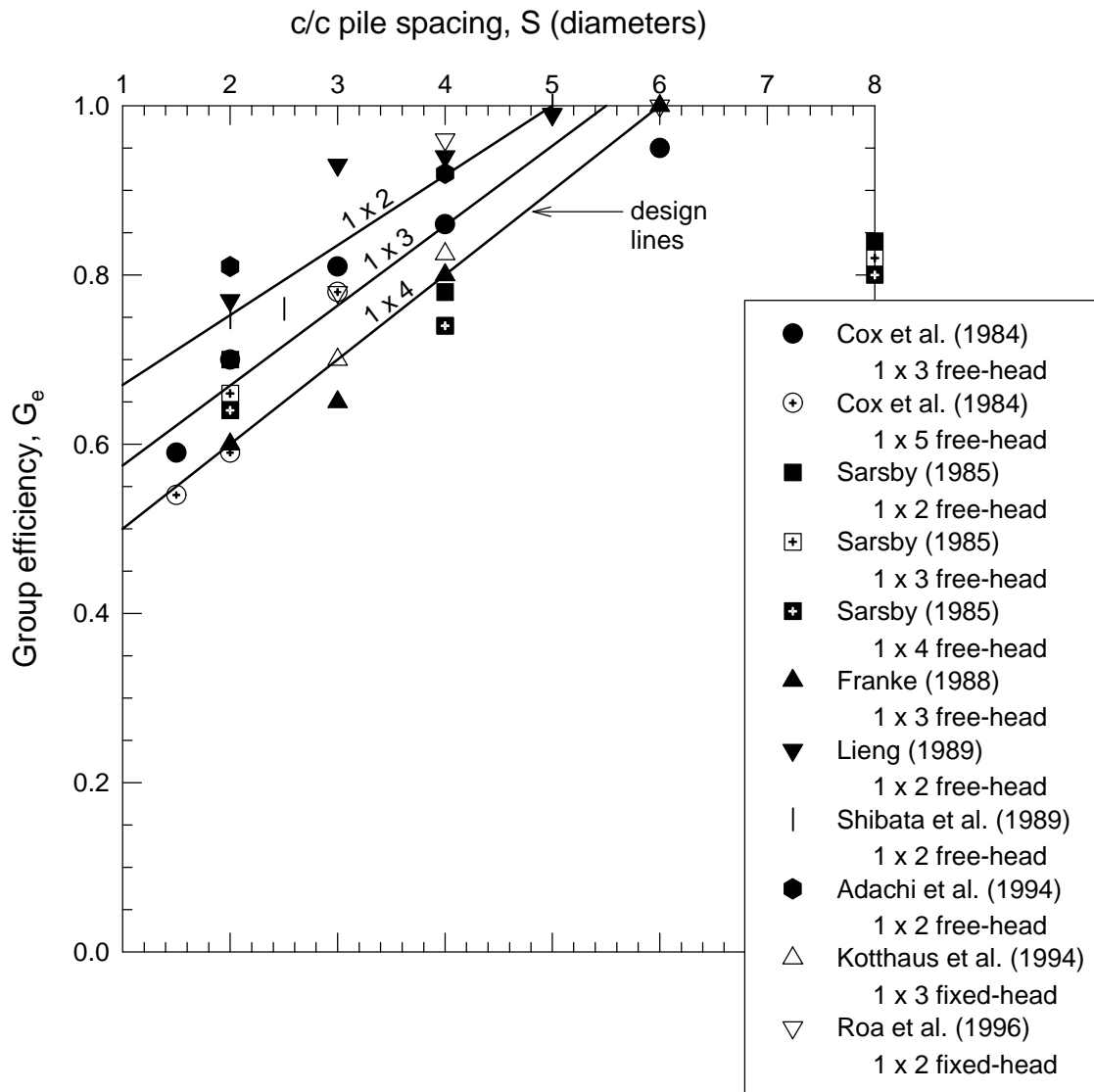


Figure 2.5. Group efficiency versus pile spacing for piles in a box arrangement.



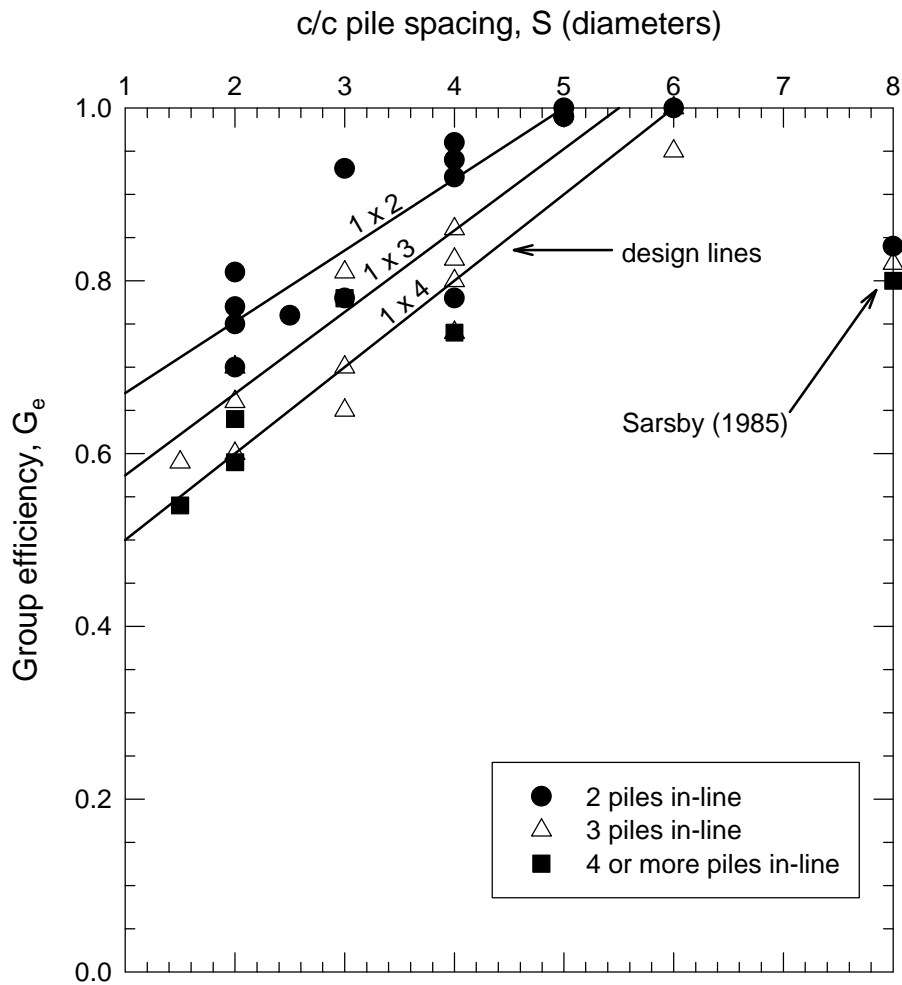
where,  $G_e = \frac{(Q_u)_g}{n(Q_u)_s}$

Figure 2.6. Influence of group size on group efficiency for piles in a box arrangement.



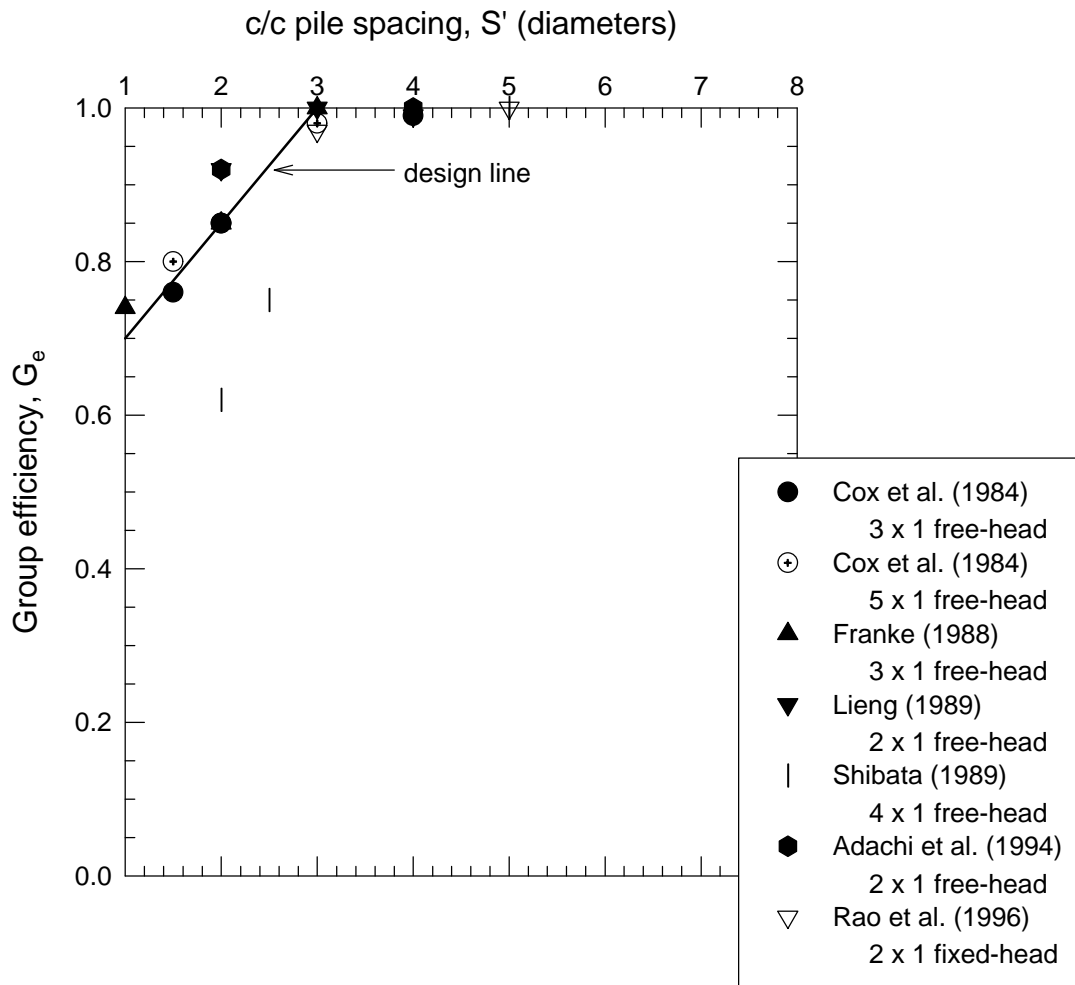
$$\text{where, } G_e = \frac{(Q_u)_g}{n(Q_u)_s}$$

Figure 2.7. Group efficiency versus pile spacing for a single row of piles oriented in the direction of load (in-line arrangement).



$$\text{where, } G_e = \frac{(Q_u)_g}{n(Q_u)_s}$$

Figure 2.8. Influence of group size on group efficiency for a single row of piles oriented in the direction of load (in-line arrangement).



$$\text{where, } G_e = \frac{(Q_u)_g}{n(Q_u)_s}$$

Figure 2.9. Group efficiency versus pile spacing for a single row of piles oriented perpendicular to the direction of load (side-by-side arrangement).

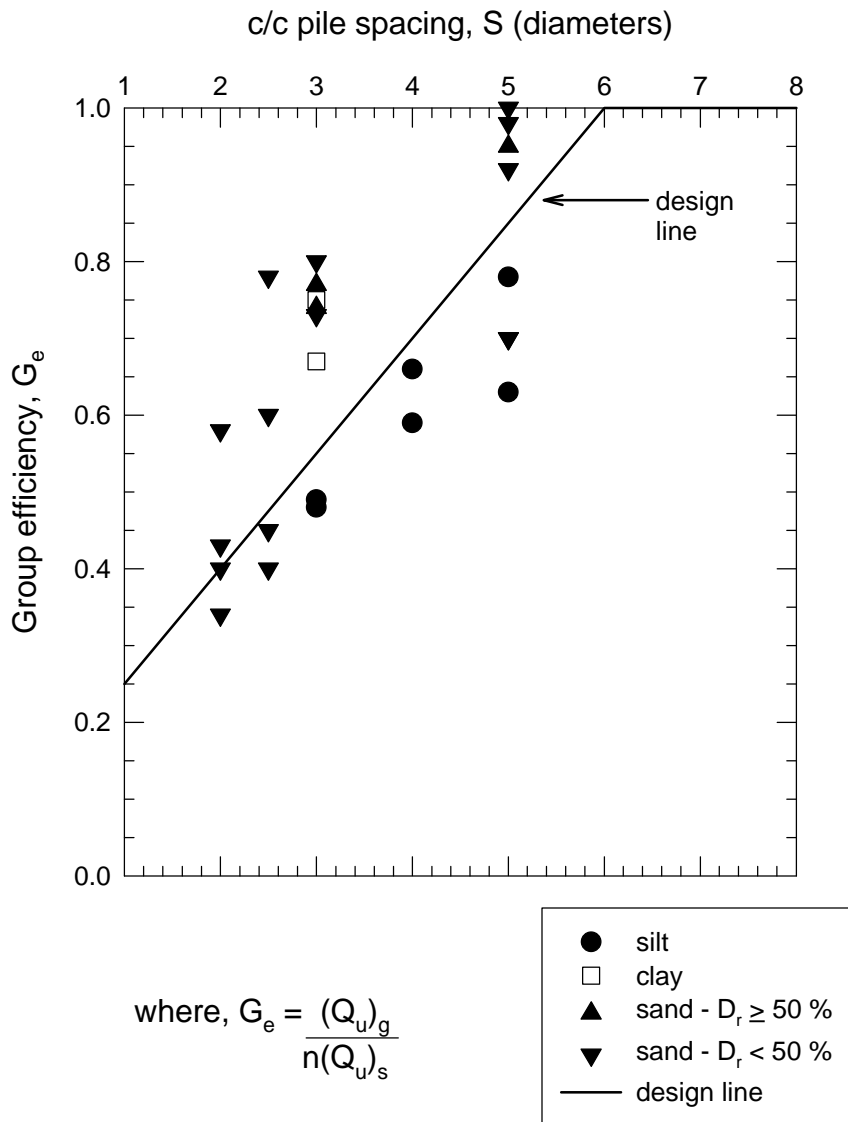


Figure 2.10. Influence of soil type on group efficiency for piles in a box arrangement.

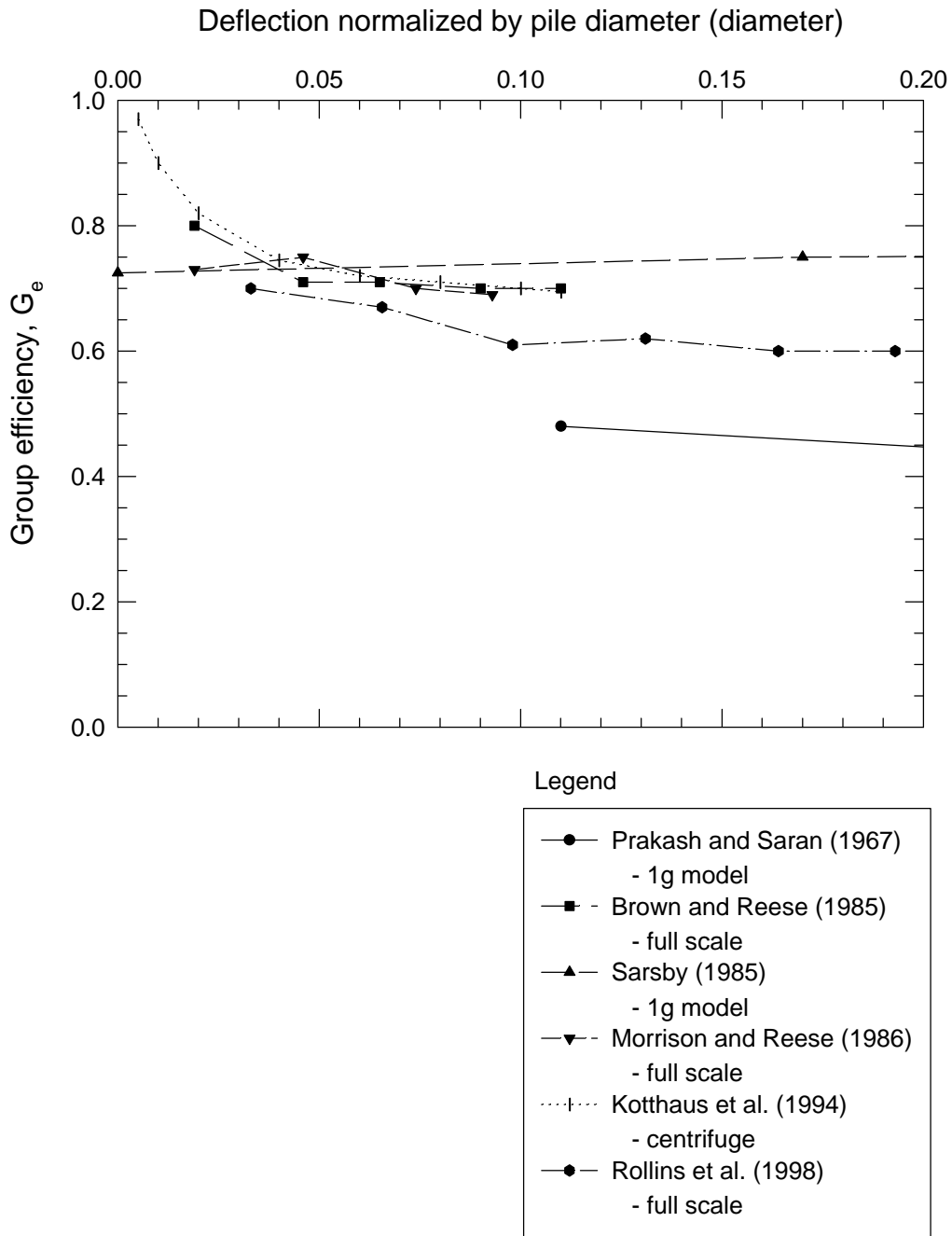
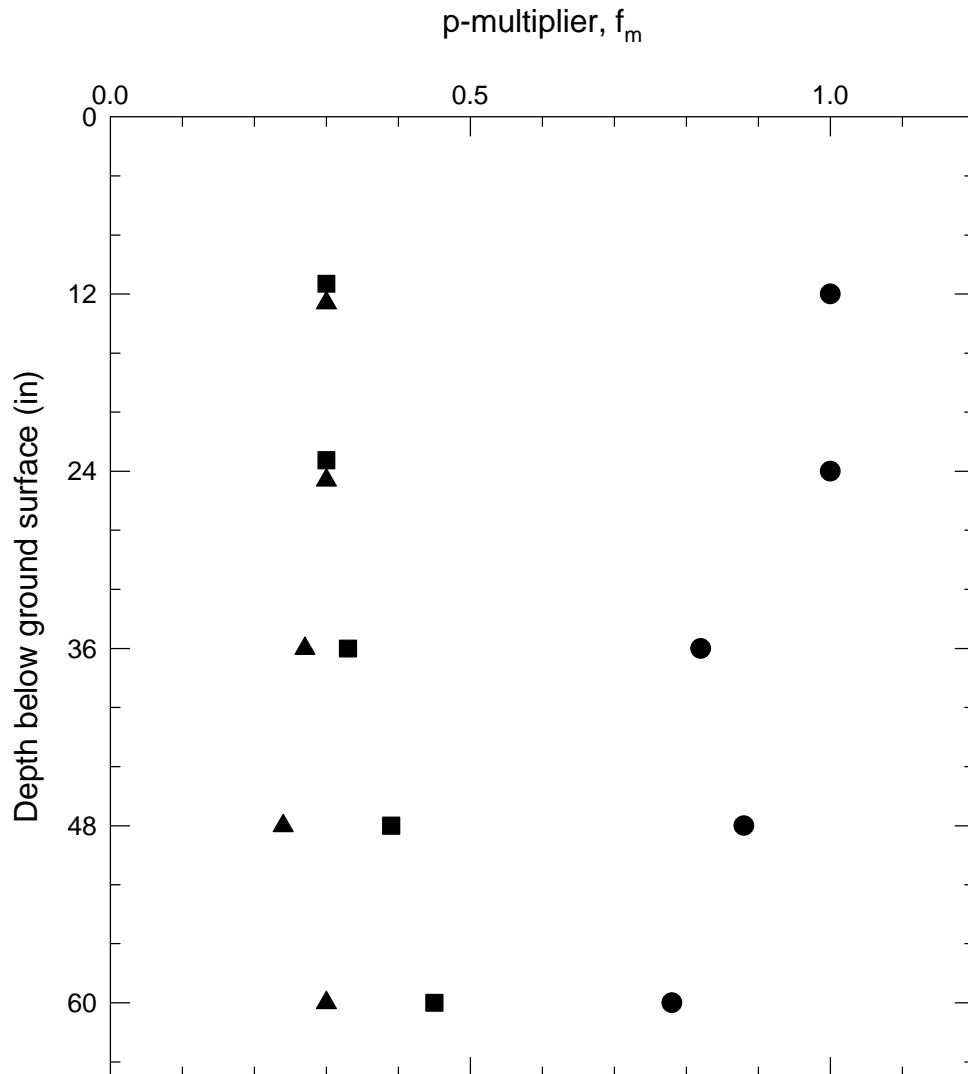


Figure 2.11. Pile group efficiency versus normalized displacement.





Experimental data obtained from full-scale field tests on a 3 by 3 pile group in sand.

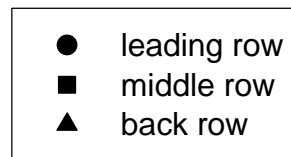


Figure 2.12. Variation of p-multiplier with depth.

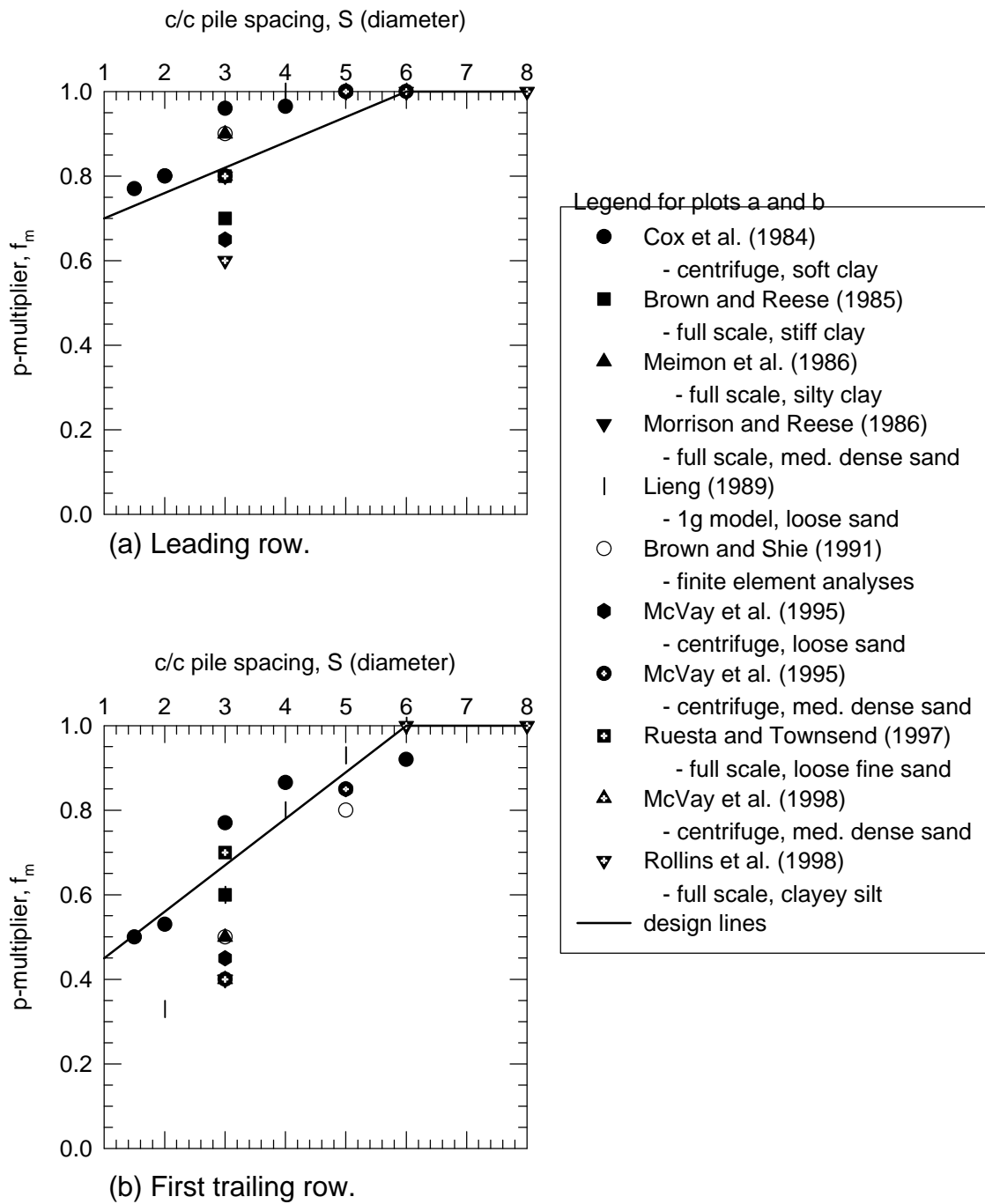


Figure 2.13. p-multiplier as a function of pile spacing for leading row and first trailing row.

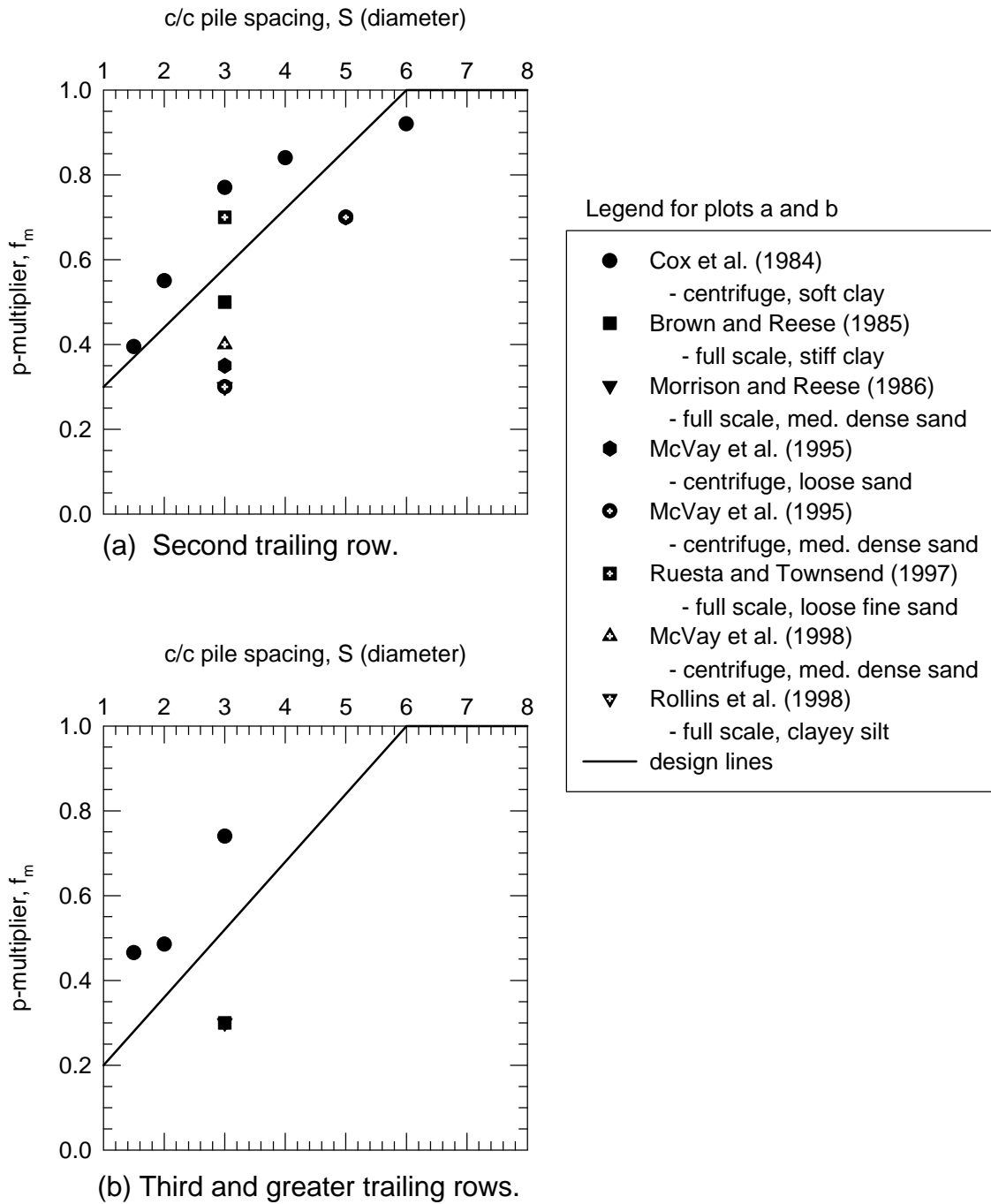
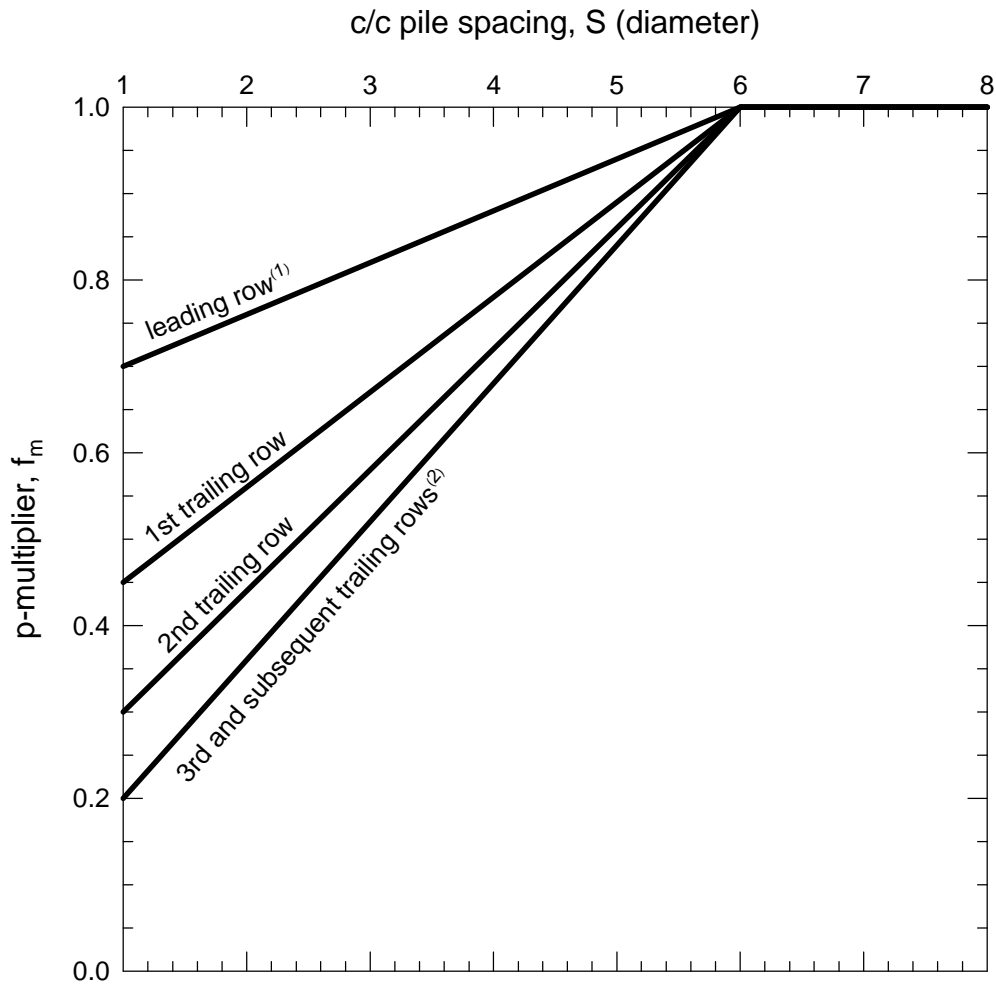


Figure 2.14. p-multiplier as a function of pile spacing for the second and third trailing rows.

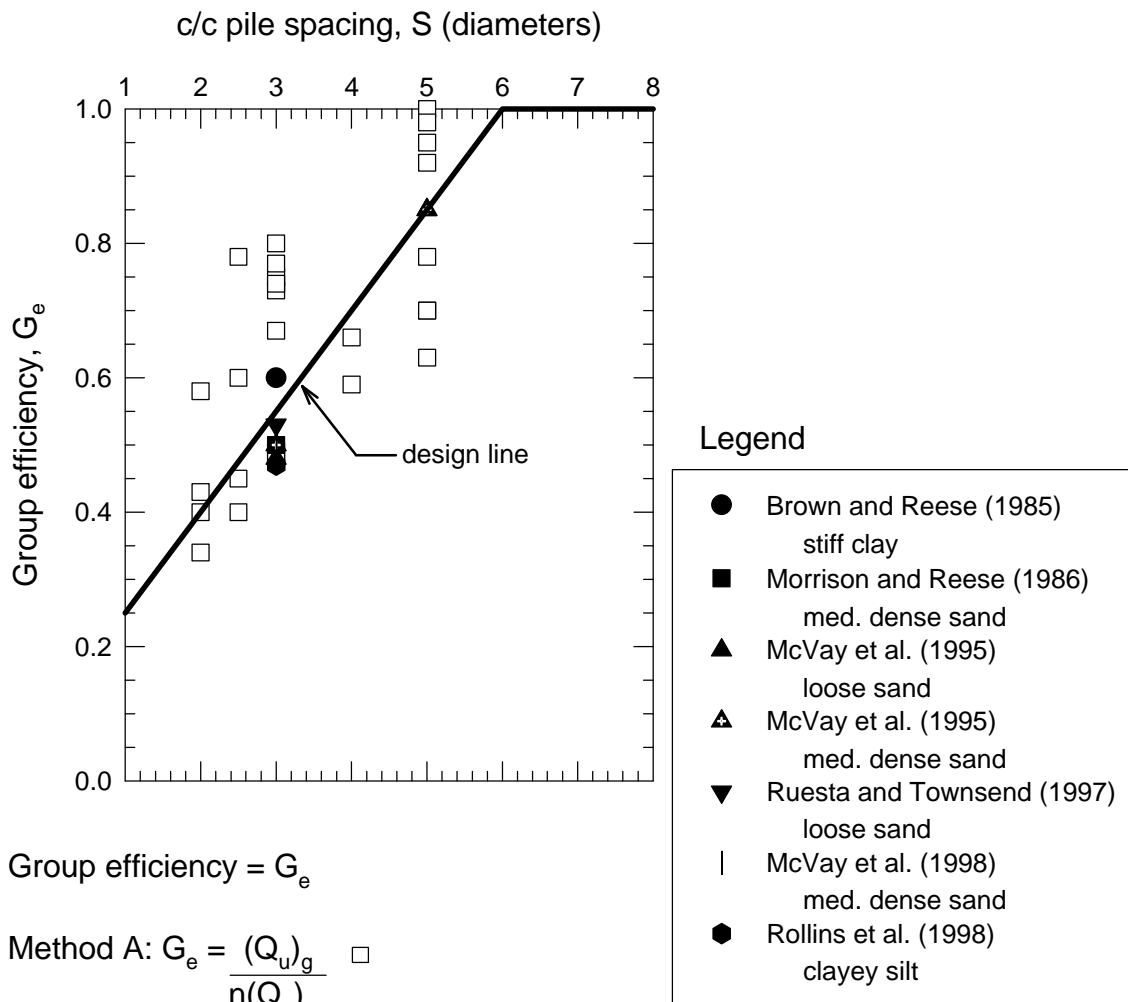


Notes:

- (1) The term row used in this chart refers to a line of piles oriented perpendicular to the direction of applied load.
- (2) Use the  $f_m$  values recommended for the 3rd trailing row for all rows beyond the third trailing row.
- (3) Bending moments and shear forces computed for the corner piles should be adjusted as follows:

<u>side by side spacing</u>	<u>corner pile factor</u>
3D	1.0
2D	1.2
1D	1.6

Figure 2.15 Proposed p-multiplier design curves.



Group efficiency =  $G_e$

Method A:  $G_e = \frac{(Q_u)_g}{n(Q_u)_s}$  □

Method B:  $G_e = \frac{\sum f_m}{N}$  ■

where,  $(Q_u)_g$  = lateral capacity of pile group at a given deflection

$(Q_u)_s$  = lateral capacity of single pile at a given deflection

$\sum f_m$  = sum of row p-multipliers

N = No. of rows in the direction of load

Figure 2.16. Proposed group efficiency design curve for piles in a square (box) arrangement.